

Serveur Académique Lausannois SERVAL serval.unil.ch

Author Manuscript

Faculty of Biology and Medicine Publication

This paper has been peer-reviewed but does not include the final publisher proof-corrections or journal pagination.

Published in final edited form as:

Title: Mild guanidinoacetate increase under partial guanidinoacetate methyltransferase deficiency strongly affects brain cell development.

Authors: Hanna-El-Daher L, Béard E, Henry H, Tenenbaum L, Braissant O

Journal: Neurobiology of disease

Year: 2015 Jul

Volume: 79

Pages: 14-27

DOI: [10.1016/j.nbd.2015.03.029](https://doi.org/10.1016/j.nbd.2015.03.029)

In the absence of a copyright statement, users should assume that standard copyright protection applies, unless the article contains an explicit statement to the contrary. In case of doubt, contact the journal publisher to verify the copyright status of an article.

Mild guanidinoacetate increase under partial guanidinoacetate methyltransferase deficiency strongly affects brain cell development

**Layane Hanna-El-Daher¹, Elidie Béard¹, Hugues Henry¹, Liliane Tenenbaum²,
Olivier Braissant¹**

¹ Neurometabolic Unit, Service of Biomedicine,

² Department of Clinical Neuroscience,

Lausanne University Hospital, CH-1011 Lausanne, Switzerland.

Correspondence to: PD Dr Olivier Braissant,

Neurometabolic Unit, Service of Biomedicine,

Lausanne University Hospital, CH-1011 Lausanne, Switzerland.

Tél : (+41.21) 314.41.52; Fax : (+41.21) 314.35.46;

e-mail: Olivier.Braissant@chuv.ch

Abstract

Among cerebral creatine deficiency syndromes, GAMT deficiency can present the most severe symptoms, and is characterized by neurocognitive dysfunction due to creatine deficiency and accumulation of guanidinoacetate in the brain. So far, every patient was found with negligible GAMT activity. However, GAMT deficiency is thought under-diagnosed, in particular due to unforeseen mutations allowing sufficient residual activity avoiding creatine deficiency, but enough guanidinoacetate accumulation to be toxic. With poorly known GAA-specific neuropathological mechanisms, we developed an RNAi-induced partial GAMT deficiency in organotypic rat brain cell cultures. As expected, the 85% decrease of GAMT protein was insufficient to cause creatine deficiency, but generated guanidinoacetate accumulation causing axonal hypersprouting and decrease in natural apoptosis, followed by induction of non-apoptotic cell death. Specific guanidinoacetate-induced effects were completely prevented by creatine co-treatment. We show that guanidinoacetate accumulation without creatine deficiency is sufficient to affect CNS development, and suggest that additional partial GAMT deficiencies, which may not show the classical brain creatine deficiency, may be discovered through guanidinoacetate measurement.

Keywords

Creatine; guanidinoacetate; creatine deficiency syndromes; GAMT deficiency; brain; development; RNA interference; adeno-associated virus.

Mild guanidinoacetate increase under partial guanidinoacetate methyltransferase deficiency strongly affects brain cell development

**Layane Hanna-El-Daher¹, Elidie Béard¹, Hugues Henry¹, Liliane Tenenbaum²,
Olivier Braissant¹**

¹ Neurometabolic Unit, Service of Biomedicine,

² Department of Clinical Neuroscience,

Lausanne University Hospital, CH-1011 Lausanne, Switzerland.

Correspondence to: PD Dr Olivier Braissant,

Neurometabolic Unit, Service of Biomedicine,

Lausanne University Hospital, CH-1011 Lausanne, Switzerland.

Tél : (+41.21) 314.41.52; Fax : (+41.21) 314.35.46;

e-mail: Olivier.Braissant@chuv.ch

Abbreviations :

AAV : adeno-associated viruses; AGAT: arginine-glycine amidinotransferase; BBB : blood-brain barrier; CNS: central nervous system; Cr : creatine; DAPI : 4',6-diamidino-2-phenylindole; EGFP : Enhanced Green Fluorescent Protein; GAA : guanidinoacetate; GABA_AR : GABA_A receptor; GAD : Glutamate Decarboxylase; GalC : Galactocerebroside; GAMT : guanidinoacetate methyltransferase; GAP43 : Growth-Associated Protein 43; GFAP : Glial Fibrillary Acidic Protein; GFP : Green Fluorescent Protein; ¹H-MRS: proton-coupled magnetic resonance spectroscopy; LC-MS/MS: liquid chromatography coupled to mass spectrometry in tandem; MAP2 : Microtubule-Associated protein 2; MBP : Myelin Basic Protein; MOI : multiplicity of infection; NeuN : Neuronal Nucleus protein; NFM : medium weight neurofilament; ORF : open reading frame; p-NFM : phosphorylated medium weight neurofilament; RNAi : RNA interference; ROC : rat hybridoma between oligodendrocytes and C6 astroglioma; scAAV : self-complementary AAV; shRNA : small hairpin RNA; SLC6A8 : creatine transporter; TUNEL : terminal deoxynucleotidyl transferase (TdT)-mediated dUTP nick end labeling.

Introduction

Deficiency of guanidinoacetate methyltransferase (GAMT), creatine (Cr) synthesis second enzyme (gene *GAMT*), was the first identified cerebral creatine deficiency syndrome (Stöckler et al., 1994; Schulze et al., 1997; Braissant, 2014; Stöckler-Ipsiroglu et al., 2014). The two other creatine deficiencies are arginine:glycine amidinotransferase (AGAT; Cr synthesis first enzyme; gene *GATM*) (Item et al., 2001) and Cr transporter (gene *SLC6A8*) (Salomons et al., 2001) deficiencies. GAMT and AGAT deficiencies are autosomal recessive inherited metabolic diseases, while SLC6A8 deficiency is X-linked. Their hallmark is the virtual Cr absence when measured by ¹H-MRS in cortex and basal ganglia. Central nervous system (CNS) is the main tissue affected, with patients developing neurological symptoms in infancy, in particular intellectual disability/developmental delay and speech acquisition defects (Schulze, 2003). GAMT deficiency can present a wide variety of symptoms from mild forms to very severe neurological phenotypes (Mercimek-Mahmutoglu et al., 2006). Guanidinoacetate (GAA) accumulation upstream of the GAMT enzymatic block is thought to cause these severe phenotypes ranging from intractable epilepsies to autistic and automutilating behaviors as well as extrapyramidal syndrome (Schulze et al., 2001; Schulze, 2003).

Unlike microcapillary endothelial cells at blood-brain barrier (BBB), surrounding astrocytes do not express SLC6A8, resulting in low Cr uptake efficiency and forcing the brain to complete its Cr needs by expressing AGAT and GAMT (Braissant et al., 2001; Béard and Braissant, 2010; Tachikawa and Hosoya, 2011; Braissant, 2012; Lowe et al., 2014). Under GAMT deficiency, cerebral Cr comes from periphery and the low BBB-crossing efficiency makes CNS Cr-deficient. Moreover, GAA accumulates in CNS (uptake from peripheral excess, endogenous AGAT

activity with no functional GAMT; Braissant, 2012). Despite low BBB Cr permeability, SLC6A8 expression in microcapillary endothelial cells allows high Cr dosage treatment of GAMT-deficient patients who nevertheless often remain with severe intellectual disability/developmental delay (Stöckler-Ipsiroglu et al., 2014). Few prenatally-diagnosed patients were treated pre-symptomatically and developed normally (Schulze and Battini, 2007; El-Gharbawy et al, 2013; Viau et al, 2013).

GAMT deficiency is treatable, potentially under-diagnosed due to limited awareness, and was thus suggested as a newborn screening candidate through GAA measure (Mercimek-Mahmutoglu et al., 2012; El-Gharbawy et al., 2013; Pasquali et al., 2014). All GAMT-deficient patients identified so far were diagnosed by ¹H-MRS-measured brain Cr deficiency and showed negligible residual GAMT activity (Mercimek-Mahmutoglu et al., 2006, 2014; Stöckler-Ipsiroglu et al., 2014; <http://www.LOVD.nl/GAMT>). Apart from identifying new patients with CNS Cr deficiency and negligible GAMT activity, newborn screening through GAA measurement may in addition identify GAMT-deficient patients with sufficient GAMT residual activity to escape diagnosis as Cr non-deficient, but sufficiently accumulating GAA to be toxic. Newborn screening may also identify other patients with levels of GAA altered independently of GAMT deficiency, as found recently for example for arginase deficiency (Amayreh et al., 2013).

While mostly known for its ATP regeneration and buffering role (Wallimann et al., 1992; Brosnan and Brosnan, 2007), Cr was recently suggested to act also as neurotransmitter (Almeida et al., 2006; van de Kamp et al., 2013). Although of poorly known pathophysiology, Cr deficiency probably affects brain energy and neurotransmission. In CNS, GAA is toxic through GABA_A receptor (GABA_AR) activation which may explain its epileptogenic action (Neu et al.,

2002), and disturbs energy through Na⁺-K⁺-ATPase/creatine kinase complex inhibition (Zugno et al., 2006). A *Gamt*^{-/-} mouse was developed showing the biochemical GAMT deficiency characteristics (Cr deficiency and GAA accumulation), which however does not present the patients severe neurological symptoms (Schmidt et al., 2004).

To better understand GAA toxicity under GAMT deficiency on developing CNS, rat organotypic 3D brain cell cultures were transduced by adeno-associated viruses (AAV) driving *Gamt* gene knock-down by RNA interference (RNAi).

Materials and Methods

Selection of GAMT shRNAs

Three 21nt siRNA sequences specific for rat *Gamt* ORF (genebank n°J03588) were selected according to the Wang and Mu (2004) algorithm and used to generate 66bp small hairpin RNA (shRNA)-encoding DNA inserts, later cloned into pRNAT-CMV3.2/Neo under cytomegalovirus (CMV) promoter (Genscript) (**Figure 1A**). GAMT-1, 2 and -3 shRNAs potential RNAi efficiency was evaluated by Dual Luciferase Assay by co-transfection of pRNAT-CMV3.2/Neo/GAMT-1/2/3/empty with psiCHECK-GAMT (Promega; vector expressing GAMT ORF downstream of *Renilla* luciferase ORF) and a control firefly luciferase-expressing vector, into ROC cells (rat hybridoma between oligodendrocytes and C6 astroglioma) plated at 80% confluence using jetPEI reagent (Polyplus). Cells were washed and lysed after 48h with lysis buffer, and cell extract was measured by Dual Luciferase Assay (Promega) using a TD-20/20 luminometer (Turner Designs). *Renilla* luciferase activity was normalized with firefly luciferase activity. GAMT-2 shRNA presented the highest RNAi potential, with 81% decrease of *Renilla* luciferase activity (**Figure 1B**). pRNAT-CMV3.2/Neo/GAMT-2, mismatched and scrambled controls were used to demonstrate the specific GAMT knock-down. After 24h, stably transfected ROC cells were selected with 300 µg/ml neomycin. Cells were harvested 6 days after transfection and their GAMT protein level was quantified by western blotting (**Figure 1C**).

Adeno-associated virus production

Several AAV genotypes/serotypes were tested to uncover the most efficient vector for developing our GAMT deficiency model in immature brain cells (Tenenbaum et al., 2004): AAV2,2/1,2/5,2/8 (single-stranded) and scAAV2,2/5,2/8,2/9 (self-complementary) with multiplicity of infection (MOI) of 100, 300 and 1000 viral genomes per cell (data not shown). AAV2 and scAAV2 proved to be the most efficient in our cultures, where they were able to target neurons, astrocytes and oligodendrocytes (**Figure 2A**). GAMT RNAi-expressing AAV2 viruses were prepared by cloning GAMT-2 shRNA and its mismatched and scrambled controls into pAAV-hrGFP (Agilent Technologies) under CMV promoter (pAAV-hrGFP/GAMT-2/mismatched/scrambled). pAAV-hrGFP co-expresses hrGFP, also under CMV promoter, for the follow-up of transduced cells. AAV2/GAMT-2/mismatched/scrambled viruses were prepared with AAV-293 cells and the Agilent AAV Helper Free system, according to supplier instructions (Agilent Technologies). Viral particles were purified with the AAV Purification Virakit according to manufacturer instructions (Virapur) and stored at -20°C until use. Titration of total AAV2 particles (empty and full viruses) was performed with the AAV2 Titration ELISA (Progen Biotechnik GMBH) according to manufacturer instructions, using a Nanodrop 2000c at 450 nm (Thermo Fisher Scientific). Titration of efficient AAV2 particles was performed by qPCR. Purified AAV2/GAMT-2/mismatched/scrambled were obtained with titers of 10^{10} . Self complementary AAV2 (scAAV2) viruses transducing GAMT RNAi were customized under the construction ITR-(U6 promoter)-(GAMT-2/mismatched/scrambled)-(CMV promoter)-EGFP-PolyA-ITR (SignaGen). EGFP allowed the follow-up of transduced cells. Purified scAAV2/GAMT-2/mismatched/scrambled were obtained with titers of 10^{12} - 10^{13} (SignaGen). AAV2/GAMT-2 particles were used to transduce ROC cells (MOI: 300) to validate the AAV2-transduced *Gamt* knock-down by GAMT-2 shRNA (**Figure 1C**), while scAAV2/GAMT-

2/mismatched/scrambled viruses were used to generate a GAMT deficiency model by transduction of GAMT-2 shRNA in 3D organotypic developing brain cell cultures in aggregates (**Figure 1D**).

3D organotypic cultures of developing brain cells

Pregnant rats (Sprague-Dawley 300g, Charles River) were handled according to the Swiss Academy for Medical Science rules. Their embryos were dissected out at E15.5 day to prepare 3D primary cultures of brain cells in aggregates from their mechanically-dissociated whole brains, as previously described (Braissant et al., 2002). Aggregates develop with neurons, astrocytes and oligodendrocytes organized in a 3D network acquiring a tissue-specific pattern resembling that of the *in vivo* brain, and are therefore considered as organotypic brain cell cultures (**Figure 2A**). They express AGAT, GAMT and SLC6A8 in the same manner as the *in vivo* brain and synthesize their own Cr, suggesting that they behave as *in vivo* CNS for Cr synthesis and transport (Braissant et al., 2001, 2008, 2010). They are grown under continuous gyratory agitation (80 rpm) in a serum-free, Cr-free and chemically-defined medium, in which precursor amino acids for GAA and Cr synthesis (Arg, Gly and Met) are provided by the DMEM amino acid mix used. To generate RNAi-driven *Gamt* knock-down, cultures were infected at day *in vitro* 0 (DIV0) by either AAV2 or scAAV2 vectors co-transducing GFP (AAV2) or EGFP (scAAV2) expression and a specific GAMT/mismatched/scrambled shRNA with MOI of 100, 300 or 1000. Additional cultures were treated, from DIV 5 on, with a final concentration of 10 or 30 μ M GAA at every medium change until harvest to verify GAA specific effects. Co-treated cultures were supplemented with 1 mM Cr with every media change until harvest. Aggregates were harvested at DIV8, 18 and 28. Aggregate pellets were collected by sedimentation, three

rapid rinsing with cold PBS, and either frozen in liquid nitrogen for metabolite (liquid chromatography coupled to tandem-mass spectrometry, LC/MS-MS) and protein (western blotting) analysis, or embedded in cryo-medium (Tissue-Tek O.C.T., Digitana) and frozen in liquid nitrogen-cooled isopentane for immunohistological analysis. Samples were kept at -80°C until use. Culture medium was also harvested at DIV8, 18 and 28 and kept at -80°C for metabolite analysis by LC/MS-MS.

Measure of creatine and guanidinoacetate

Cr and GAA determination in 3D cultures was performed by LC/MS-MS, as described in details (Braissant et al., 2008). For intracellular measure, aggregates were homogenized in 0.1 % (v/v) formic acid in H₂O at 4°C using a FastPrep Cell Disrupter F120 (Qbiogene) and centrifuged at 10'000 g for 5 min at 4°C. To 20 µl of the supernatant were successively added 5 µl of 10 µM d₃-Cr (CDN Isotopes) and 10 µM ¹³C₂-GAA (CDN Isotopes) as internal standards, 171 µl H₂O and 4 µl formic acid (98-100 % w/v). For extracellular measure, 20 µl of culture medium were used. Cr and GAA were purified by micro-solid phase extraction (Oasis MCX µElution Plate, Waters). Separation of Cr and GAA was achieved at 30°C using an ACQUITY® UPLC BEH HILIC silica 2.1x50mm 1.7µm column (Waters). The column flow rate was 300 µl/min and the mobile phases consisted of acetonitrile, H₂O and 200 mmol/l ammonium formate pH 3.2. The column effluent was monitored using a Triple Quadrupole TSQ Quantum Discovery (Thermo Scientific). The instrument was equipped with an electrospray interface and controlled by the Xcalibur software (Thermo Scientific). Samples were analyzed in positive ionization mode operating in a cone voltage of 4kV. The tandem mass spectrometer was programmed using the selected

reaction monitoring mode (SRM) to allow the $[MH^+]$ ions of Cr and GAA respectively at m/z 132 and 118 and that of the internal standards D_3 -Cr and $^{13}C_2$ -GAA at m/z 135 and 120 to pass through the first quadrupole (Q1) and into the collision cell (Q2). The daughter ions for Cr and GAA were of m/z 90 and 76 respectively, and of m/z 93 and 78 for D_3 -Cr and $^{13}C_2$ -GAA respectively. Calibration curves were computed using the ratio of the peak area of the analytes and internal standard using a weighted ($1/x^2$) least squares linear-regression analysis.

Antibodies, western blotting and immunohistochemistry

The GAMT protein was detected with an affinity-purified rabbit polyclonal antibody previously developed in our laboratory and used with a 1:1000 concentration (Braissant et al., 2005). All the other primary antibodies used in this study are commercially available, as follows: GalC (1:100, MAB5254), GFAP (1:100/1:5'000, MAB 360), MAP-2 (1:100, MAB378), NeuN (1:100, MAB377), p-NFM (clone NN18, 1:100, MAB5254) and GABA_AR (1:100/1:500, MABN489, targeting the $\alpha 1$ subunit of GABA_AR) mouse monoclonal and GAP43 (1:100/1:20'000, AB5220) rabbit polyclonal (Chemicon); β -tubulin (1:1'000, T8578) mouse monoclonal (Sigma-Aldrich); Actin (1:1'000, sc1616), MBP (1:500, sc13914) and GAD (1:100/1:500, sc7513) goat polyclonal; NFM (clone NF-09, 1:1'000, sc51683) mouse monoclonal (Santa Cruz Biotechnology); cleaved caspase-3 (1:200, 9664) and caspase-3 (1:1'000, 9665) rabbit monoclonal (Cell Signaling Technology). Secondary antibodies were horse radish peroxidase-conjugated goat anti-mouse, anti-rabbit or rabbit anti-goat IgG (Vector laboratories) for western blotting, and goat anti-mouse, anti-rabbit or donkey anti-goat IgG labeled with Alexa Fluor® 555 (red) (Life Technologies).

For western blotting, brain cell aggregates or ROC cells were homogenized in 150 mM NaCl, 50 mM Tris-HCl, pH 8.0, 1% NP-40 (Sigma-Aldrich) and Protease Inhibitor Cocktail - Complete Mini (Roche), sonicated and centrifuged. The supernatant was harvested and protein dosage was performed by bicinchoninic acid assay (Thermo Scientific). Samples were prepared with a final concentration of 1 $\mu\text{g}/\mu\text{l}$ in NuPAGE[®] LDS Sample Buffer and resolved on NuPAGE[®] 4-12% or 12% Bis-Tris gels using NuPAGE[®] MOPS SDS Running Buffer (Life Technologies) at a constant voltage (200 V, 60 min). Protein transfer was then performed on nitrocellulose membranes (Millipore) for 1h at 100 V. Membranes were washed in TBS/Tween (20 mM Trizma base, 137 mM NaCl, 0.05% Tween, pH 7.6) and blocked in 5% non-fat dry milk in TBS-Tween for 1h at RT. Membranes were incubated with primary antibodies (see above) diluted in 3% dry milk and TBS-Tween, O/N at 4°C. Membranes were probed with horse radish peroxidase-conjugated secondary antibodies (see above) diluted 1:3000 in 3% dry milk and TBS-Tween, 2h at RT, then developed by chemiluminescence (ECL Western Blotting Detection Reagents, GE Healthcare). Blots were stripped (ReBlot Plus Mild Antibody Stripping Solution, Millipore) and re-probed with antibody against β -tubulin or actin as loading control. Images were taken with a Luminescent Image Analyzer LAS-4000 (Fujifilm, Life Science) and quantified with the public Java-based image processing program ImageJ (National Institutes of Health). Data were acquired in arbitrary densitometric units and transformed to percentages of the densitometric levels of control samples visualized on the same blots.

For immunohistochemistry, 16 μm cryosections of aggregates were fixed 1h in 4% paraformaldehyde in PBS at RT. Non-specific antibody binding sites were blocked 1h at RT with 1% bovine serum albumin (BSA; Sigma-Aldrich) in PBS (BSA-PBS). Primary antibodies diluted

1:100 in 1% BSA-PBS where applied to sections O/N at 4°C, then detected with appropriate fluorescent secondary antibodies (1:100, 2h RT) labeled with Alexa Fluor® 555 (see above). Tyramide Signal Amplification (TSA, Molecular Probes) was used to amplify the detection signal of cleaved caspase-3, according to supplier recommendations. Sections were mounted under FluorSave Reagent (Calbiochem) and observed using an Olympus BX50 microscope equipped with appropriate filters for red, green and blue fluorescence. Stained sections were digitized with a UC30 digital camera mounted on the microscope, allowing image processing and merging with the Cell Sens Imaging Software (Olympus).

Evaluation of cell death

Cell death in our cultures was evaluated through three different techniques. Apoptosis was evaluated by western blotting and immunohistochemistry for activated cleaved caspase-3 (red fluorescence). Cryosections stained for cleaved caspase-3 were co-labeled by terminal deoxynucleotidyl transferase (TdT)-mediated dUTP nick end labeling (TUNEL, green fluorescence, Roche Applied Science) and nuclear 4',6-diamidino-2-phenylindole (DAPI, blue fluorescence, Life technologies) staining according to suppliers recommendations, in order to evaluate the proportions of apoptotic and non-apoptotic cell deaths.

Evaluation of GAMT RNAi specificity in 3D organotypic brain cell cultures

GAMT RNAi specificity in 3D brain cell cultures was analyzed by the use of negative controls, evaluation of off-target effects, as well as direct GAA exposure and Cr rescue experiments. Empty scAAV2 vectors (i.e. expressing EGFP but not transducing any shRNA), as well as

scAAV2 vectors transducing specific mismatched and scrambled controls for GAMT-2 shRNA, were used as negative controls, always with the maximal MOI of 1000. Using these negative controls, no significant effect on GAMT protein expression or Cr and GAA levels could be observed. The mismatched control, having 2 mutations in the middle of the GAMT-2 siRNA sequence and thus showing very similar hybridization properties, allowed evaluation of off-target effects. scAAV2/mismatched-transduced cultures showed no significant differences as compared to control or scAAV2/empty-transduced cultures. In particular, no significant effect on culture growth, brain cell morphologies or death were observed, nor on the expression of genes involved in cytoskeleton (NFM, p-NFM, MAP2, GFAP, actin, β -tubulin), myelin sheath (MBP), neurotransmission (GAD, GABA_AR) or apoptosis (caspase-3). The specificity of GAA effects under GAMT RNAi was verified by direct exposure to 10 and 30 μ M GAA, which resumes the effects of scAAV2-transduced GAMT RNAi. Finally, rescue experiments by Cr co-treatment (1 mM) prevented every effect of GAMT RNAi, or of direct GAA exposure, observed in this study, in particular by preventing GAA accumulation despite GAMT deficiency. This demonstrated that every RNAi-driven effect observed in this study were specifically due to GAA accumulation (**Figures 3-7**).

The only non-specific effect shown in this study was due to scAAV2 vectors, and not to RNAi. Indeed, scAAV2 drove a non-specific reactive effect in 3D brain cell cultures that was observable only on the long term (DIV28), in particular by reactive astrocytes (GFAP increase), slowing of oligodendrocyte differentiation (MBP decrease but stability of GalC) and decrease of NFM (**Figures 4,5**).

Statistical analysis

All data points are expressed as mean \pm standard error of the mean (SEM). Statistical significance of the differences between various conditions was determined by Student's *t*-test (one way analysis of variance); $p < 0.05$ was considered significant. Data from 3D organotypic brain cell cultures are representative of more than 5 independent culture settings, each performed with $n=6$ for each conditions. Within these culture settings: Cr/GAA measurements by LC/MS-MS representative of 3 independent experiments, evaluated with $n=6$ for each conditions; histological data representative of 4 independent experiments, evaluated with $n=3$ for each conditions; western blotting representative of 4 independent experiments, evaluated with $n=3$ for each conditions.

Results

scAAV2-transduced GAMT deficiency in developing brain cells

Three rat *Gamt* open reading frame (ORF)-specific sequences were selected (**Figure 1A**) and used in GAMT-expressing ROC cells to evaluate their RNAi potential by dual luciferase assay. Maximal RNAi was obtained by GAMT-2 shRNA (-80%; **Figure 1B**). RNAi specificity was analyzed by ROC cells transfection with pRNAT-CMV3.2/Neo/GAMT-2, mismatched/scrambled controls (**Figure 1A**) and empty vectors. GAMT-2 shRNA led to a 85% GAMT protein decrease (**Figure 1C**). GAMT expression after empty/mismatched/scrambled transfections was not significantly different from untransfected cells.

Having determined the best interfering sequence in nerve cell monolayer (**Figure 1A-C**), our next goal was choosing the best AAV to maximize 3D brain cell cultures transduction (**Figure 2A,B**). Many serotypes exist with transduction efficacy depending on cellular tropism and models used. Therefore, several genotypes/serotypes were tested (AAV2,2/1,2/5,2/8; scAAV2,2/5,2/8,2/9) with MOI of 100, 300 and 1000, uncovering the most efficient for our model. AAV exposure was initiated at DIV0 to maximize infection before cell aggregation. AAV2/scAAV2 proved to be the best (data not shown), and transduced neurons, astrocytes and oligodendrocytes as shown by Enhanced Green Fluorescent Protein (EGFP) expression observable from DIV5 to 28, co-labeled with Neuronal Nucleus protein (NeuN), Glial Fibrillary Acidic Protein (GFAP) and Galactocerebroside (GalC) respectively; **Figure 2B**). AAV2-driven GAMT-2 shRNA expression was tested in ROC cells (MOI: 300) leading to 75% GAMT protein decrease (**Figure 1C**).

To generate a GAMT-deficient model in developing CNS, scAAV2/GAMT-2/mismatched/scrambled were transduced in 3D organotypic brain cell cultures (**Figure 1D,E**). MOIs 100/300/1000 were tested, except for mismatched/scrambled which received MOI 1000 only. The GAMT protein decrease was significant, maximal and attenuated at DIV8, 18 and 28, respectively (-37±9%; -85±10%; -50±14%; MOI 1000) (**Figure 1D**). At DIV8, controls expressed low GAMT levels (6% of DIV18; **Figure 1E**), and mild RNAi was observed (-46%). Maximal GAMT levels were observed in DIV18 controls, in which knockdown was as efficient as -94% in this representative culture (**Figure 1E**). GAMT was less expressed at DIV28 (78% of DIV18; **Figure 1E**), where a maximal -75% knockdown was induced.

No creatine deficiency but guanidinoacetate accumulation under partial GAMT deficiency

Despite significant GAMT protein knockdown at DIV8 (-37%), DIV18 (-85%) and DIV28 (-50%) (**Figure 1D**), no Cr deficiency was observed in scAAV2/GAMT-2-transduced cultures. Cr, analyzed by liquid chromatography coupled to mass spectrometry in tandem (LC-MS/MS), was measured intracellularly at 61±6 *versus* 75±14 nmol*mg prot⁻¹ in controls *versus* scAAV2/GAMT-2 cultures at DIV8, 249±41 *versus* 227±22 nmol*mg prot⁻¹ at DIV18, and 258±30 *versus* 219±33 nmol*mg prot⁻¹ at DIV28 (**Figure 3A**). Extracellular Cr levels were measured at 1.1±0.2 µM *versus* 1.2±0.1 µM in controls *versus* scAAV2/GAMT-2 cultures at DIV8, 20.6±0.3 *versus* 23.6±1.1 µM at DIV18, and 17.8±2.1 *versus* 25.3±3.2 µM at DIV28 (**Figure 3A**). No significant difference in scAAV2/mismatched/scrambled cultures was observed. scAAV2/GAMT-2 cultures co-treated with 1mM Cr showed increase of both intracellular (508±27, 340±37 and 322±28 nmol*mg prot⁻¹) and extracellular (533±34, 558±35

and $876 \pm 92 \mu\text{M}$) Cr at DIV8, 18 and 28 respectively (**Figure 3A**). Co-treating cultures with Cr to prevent GAMT knockdown deleterious effect was performed at each medium renewal, Cr being measured prior to both medium change and next Cr co-treatment.

As anticipated however, GAMT knockdown caused GAA accumulation which, analyzed by LC-MS/MS, was increased intracellularly compared to controls at DIV8 (14.9 ± 1.4 versus 2.8 ± 0.7 $\text{nmol} \cdot \text{mg prot}^{-1}$) and 18 (45.7 ± 2.0 versus 4.0 ± 1.2 $\text{nmol} \cdot \text{mg prot}^{-1}$) (**Figure 3B**). Extracellular GAA levels followed identical patterns (DIV8: 1.5 ± 0.1 versus $0.5 \pm 0.1 \mu\text{M}$; DIV18: 9.0 ± 0.9 versus $0.9 \pm 0.3 \mu\text{M}$) (**Figure 3B**). At DIV28, GAA was barely detectable (intracellular: 0.6 ± 0.1 versus 0.7 ± 0.1 $\text{nmol} \cdot \text{mg prot}^{-1}$; extracellular: 0.2 ± 0.1 versus $0.2 \pm 0.1 \mu\text{M}$). At all stages, no significant difference in scAAV2/mismatched/scrambled cultures was observed, except with DIV18 scAAV2/scrambled (slight GAA increase; data not shown). Interestingly, GAA accumulation was prevented with Cr co-treatment, with lower GAA levels than in controls (intracellular: 1.3 ± 0.1 versus 2.8 ± 0.7 $\text{nmol} \cdot \text{mg prot}^{-1}$ at DIV8; 1.2 ± 0.5 versus 4.0 ± 1.2 $\text{nmol} \cdot \text{mg prot}^{-1}$ at DIV18; extracellular: 0.4 ± 0.1 versus $0.5 \pm 0.1 \mu\text{M}$ at DIV8; 0.4 ± 0.1 versus $0.9 \pm 0.1 \mu\text{M}$ at DIV18).

Partial GAMT deficiency generates axonal hypersprouting

To investigate GAMT RNAi-induced consequences on developing neurons, we analyzed scAAV2/GAMT-2-transduced cultures for neuron-specific markers. The most striking observation was a specific axonal hypersprouting, shown by the strong increase of axonal-enriched phosphorylated medium weight neurofilament (p-NFM; **Figure 4A,B**). Axonal bundles

augmentation was already observed at DIV8, but was most striking at DIV18, accompanied by axonal fibers and branches disorganization, developing in all directions including in aggregates center, otherwise peripherally-restricted (**Figure 4A**; see also **Figure 2A**). GAMT RNAi-induced total (3.6x) and phosphorylated (4.4x) NFM increase was confirmed by western blot (DIV18; **Figure 4B**). Axonal hypersprouting was also confirmed by the growth cone marker Growth-Associated Protein 43 (GAP43) augmentation (1.8x at DIV18; **Figure 4B**). At DIV8 and 18, Cr co-treatment prevented axonal hypersprouting (**Figure 4A,B**). In neurons, GAA preferentially affected axons, as no significant effect was observed on Microtubule-Associated protein 2 (MAP2; neuronal soma and dendrites; DIV18; **Figure 4C**). At DIV28, axonal hypersprouting was still present (p-NFM, **Figure 4A**; 1.9x GAP43 increase, **Figure 4B**). However, holes in aggregates centers were noticed (asterisks; **Figure 4A**), suggesting a secondary GAA-induced neuronal death illustrated by total (-46%) and phosphorylated (-40%) NFM decrease (**Figure 4B**). At DIV28, Cr co-treatment also prevented GAMT RNAi-induced effects on neurons (**Figure 4A**). However, NFM levels were lower in Cr-co-treated cultures than controls (**Figure 4A,B**), and at similar levels compared to scAAV2/mismatched/scrambled aggregates. In contrast to younger stages (DIV8,18), this suggests a viral effect on the long-term (see **Figure 5** for similar effects on glial cells). We conclude that partial GAMT deficiency did not affect neuronal soma or dendrites but led to axonal hypersprouting that Cr co-treatment could prevent.

Partial GAMT deficiency does not affect glial cells

To investigate GAMT RNAi-induced glial cell disturbances, we analyzed scAAV2/GAMT-2-transduced cultures for glial-specific markers. No GAMT RNAi-induced consequence on developing astrocytes was noticed at DIV8 and 18, confirmed by GFAP expression (**Figure**

5A,B). Oligodendrocytes followed the same outcome, as validated by GalC and Myelin Basic Protein (MBP) expression (**Figure 5C,E**). Cr co-treatment did not affect GFAP or GalC (**Figure 5A-C**). At DIV28, apart from the holes observed in aggregates centers, no GAMT RNAi-specific glial effect was observed (**Figure 5A,C**). However, as for neurons (**Figure 4**), a viral effect was seen at DIV28, with GFAP increase and MBP decrease in every scAAV2-transduced culture (**Figure 5A,B,D,E**), suggesting a long-term scAAV2-induced astrocyte reactivity and oligodendrocyte differentiation delay.

Partial GAMT deficiency secondarily generates non-apoptotic cell death

Axonal hypersprouting (DIV8, 18) and tissue loss (DIV28) (**Figures 4,5**) suggest that GAMT RNAi may alter natural brain cell death and drive tissue damage. We therefore investigated cell death by triple fluorescent co-staining of cleaved caspase-3 (apoptosis; red), TUNEL (all cell deaths; green) and DAPI (nucleus; blue) (**Figure 6A**). Apoptosis occurs in developing 3D brain cell aggregates as in immature CNS (Honegger and Monnet-Tschudi, 2001; Cagnon and Braissant, 2008) with higher cell death in younger compared to mature stages (red staining in control aggregates center) (**Figure 6A**). For all stages, we showed similar amounts of cell death in untreated and scAAV2/mismatched/scrambled-transduced cultures, thus excluding viral toxicity. Interestingly, scAAV2/GAMT-2-induced RNAi caused a significant natural apoptosis decrease, shown by cleaved caspase-3 reduction at DIV8, 18 and 28 (44%, 61% and 64%, respectively) which was prevented by Cr supplementation (**Figure 6A,B**). Moreover, cell death pattern was modified at DIV28 with a significant increase of TUNEL-only positive cells in scAAV2/GAMT-2-transduced aggregates centers (**Figure 6A**), suggesting a GAMT RNAi-induced secondary induction of non-apoptotic cell death. Interestingly, these TUNEL-positive

cells surrounded the tissue loss observable as holes in scAAV2/GAMT-2-transduced aggregate centers (**Figure 6A**, asterisks) and could also be prevented by Cr supplementation.

Direct exposure to GAA specifically resumes the effects of partial GAMT deficiency

To investigate whether the observed GAMT RNAi-induced disturbances on axonal growth and cell death were specific of GAA accumulation, we exposed the 3D brain cell aggregates to GAA at 10 and 30 μ M from DIV5 on, neighboring the extracellular GAA concentrations reached by scAAV2/GAMT-2 knockdown at DIV18 (see **Figure 3**). At DIV18, a dose-dependent axonal hypersprouting was observed under direct GAA exposure, while Cr supplementation prevented this effect for both 10 and 30 μ M GAA (**Figure 7A**). Cell death analysis under direct GAA exposure revealed a similar effect as with scAAV2/GAMT-2 knockdown, showing at DIV18 a strong dose-dependent inhibition of apoptosis (cleaved caspase 3; red) and a complete inhibition of non-apoptotic cell death (TUNEL; green), which were also prevented by Cr co-treatment (**Figures 7B**). These results strongly suggest that GAA accumulation specifically and directly drives the effects on axonal growth and cell death in our model of partial GAMT deficiency in developing brain cells by RNAi.

As GAA accumulates intracellularly under scAAV2/GAMT-2 knockdown while direct GAA application is extracellular, intra- and extracellular levels of GAA were measured at DIV8 and 18 to verify that extracellularly-applied GAA at 10 and 30 μ M was indeed taken up by brain cells (**Figure 7C**).

At DIV8, intracellular levels of GAA were increased under both 10 and 30 μM GAA exposure (3.3 ± 0.7 and 20.2 ± 1.8 *versus* 1.3 ± 0.1 $\text{nmol}\cdot\text{mg prot}^{-1}$, $p<0.01$ and $p<0.001$ respectively) (**Figure 7C**). GAA was not detectable in the medium of control cultures, while extracellular GAA levels under 10 and 30 μM GAA exposure were decreased to 0.53 ± 0.12 and 3.91 ± 0.43 μM respectively at DIV8 (**Figure 7C**). Similar results were obtained at DIV18. While intracellular GAA remained low under 10 μM GAA exposure (respectively 0.30 ± 0.04 and 0.40 ± 0.10 $\text{nmol}\cdot\text{mg prot}^{-1}$), it was increased under 30 μM GAA exposure (7.3 ± 3.4 $\text{nmol}\cdot\text{mg prot}^{-1}$, $p<0.01$ as compared to controls) (**Figure 7C**). GAA was undetectable extracellularly in DIV18 control cultures, while extracellular GAA levels under 10 and 30 μM GAA exposure were decreased to undetectable and 2.55 ± 0.86 μM respectively at DIV18 (**Figure 7C**). Our data confirm that externally-applied GAA is efficiently taken up by brain cells, even at much lower concentrations than previously published in the same system (10 / 30 μM *versus* 200 / 1000 μM) (Braissant et al 2010).

Altogether, our findings under direct GAA exposure confirm that the observed axonal hypersprouting and cell death disturbances are directly linked to the GAA accumulation caused by scAAV2/GAMT-2 knockdown in our partial GAMT deficiency model.

GAA accumulation specifically alters GABAergic pathways

As GAA activates GABA_AR (Neu et al., 2002), we investigated whether its GAMT RNAi-induced accumulation could disturb genes of the GABA-ergic neurotransmission pathway and whether Cr supplementation could prevent this effect. The expression of the presynaptic enzyme

Glutamate Decarboxylase (GAD, GABA synthesis) and of the postsynaptic receptor GABA_AR were significantly increased in GAMT RNAi cultures (DIV18 and 28; **Figure 8**). In control conditions, GAD expression was restricted to neuronal cell bodies located in aggregate centers (**Figure 8A**, arrows), while under GAMT RNAi increased levels were also peripherally-located in the dense fiber zone. GABA_AR was more widespread in control conditions (**Figure 8B**). However, as for GAD, GAMT RNAi induced a GABA_AR increase in peripheral fibers, which was prevented by 1 mM Cr co-treatment (**Figure 8**).

Discussion

Since its discovery (Stöckler et al., 1994; Schulze et al., 1997; Braissant, 2014; Stöckler-Ipsiroglu et al., 2014), research on GAMT deficiency aimed at improving existing treatments (Cr supplementation; better means to decrease GAA). GAA accumulation in CNS is thought to cause its specific but poorly known pathophysiology. The only existing model, the *Gamt*^{-/-} mouse, while showing biochemical hallmarks (CNS Cr deficiency and GAA accumulation), does not present the severe neurological symptoms observed in patients (Renema et al., 2003; Schmidt et al., 2004; Tran et al., 2014).

3D organotypic brain cell cultures in aggregates to model GAMT deficiency

We chose 3D organotypic brain cell cultures to better understand GAMT deficiency in developing CNS (Honegger and Monnet-Tschudi, 2001; Braissant et al., 2002). They are derived from embryonic rat brains, grown in a chemically-defined medium without serum and Cr, develop in a stereotyped fashion (**Figure 2A**) and express AGAT, GAMT and SLC6A8 as the *in vivo* CNS (Braissant et al., 2001, 2008, 2010; Tachikawa et al., 2004; Lowe et al., 2014). To generate gene knockdown, we chose AAV vectors, known to cause little pathogenicity, offering many serotypes and cellular tropism and allowing post-mitotic cell transduction (Cearley et al., 2008). In our cultures, scAAV2 targeted neurons, astrocytes and oligodendrocytes and induced GAMT deficiency by transducing a specific GAMT shRNA. No significant off-target effect could be observed (see **Materials and Methods**).

While scAAV2/GAMT efficiently drove RNAi, *Gamt* knock-down was incomplete (15% mean residual protein expression) and insufficient to cause Cr deficiency, but generated GAA accumulation, most probably by decrease of the Cr synthesis flux through partial GAMT activity in presence of normal AGAT expression. The mild GAA accumulation obtained in our model was comparable to GAA levels observed in GAMT-deficient patients cerebrospinal fluid (Almeida et al., 2004; Braissant and Henry, 2008; Stöckler et al., 2014). This allowed analysis of GAA-specific effects on brain cell development independently from Cr deficiency. Our study is the first demonstrating endogenous GAA accumulation by GAMT-deficient brain cells. The transient scAAV2-driven GAMT RNAi effect in our cultures (DIV18: maximal knock-down; DIV28: no more GAA accumulation) allowed demonstrating the potential irreversible impact of transient brain cell exposure to GAA.

Our main finding was GAA-induced neuronal differentiation disturbance. Important axonal hypersprouting was observed early and peaked at DIV18, while no other morphological neuronal alterations were noticed. A decrease of apoptotic cells in aggregates centers, known to be neurons undergoing normal developmental cell death (Honegger and Monnet-Tschudi, 2001; Cagnon and Braissant, 2008), accompanied axonal hypersprouting, suggesting a GAA-induced dysregulation disengaging neurons from apoptosis and overstimulating them to elongate axons. The specificity of the GAA-induced deleterious effects on brain cell development under GAMT knockdown was confirmed by the strict reproducibility of these effects under direct GAA exposure.

No specific GAA-linked consequence was observed on glial cells. However, a non-specific long-term viral effect was seen at DIV28 through astrocytic reactivity (GFAP increase) and slowing of oligodendrocytes differentiation (stable GalC but MBP decrease).

Relevance to GAMT deficiency and potential mechanisms

GAMT deficiency results in intellectual disability/developmental delay, speech acquisition impairment, autistic behavior, severe epilepsies and movement disorders (Stöckler-Ipsiroglu et al., 2014). During normal development, synaptogenesis requires initial neuronal apoptosis inhibition, exuberant axonal growth, and postsynaptic neuronal targeting followed by selective axonal pruning (Low and Cheng, 2006; Diez et al., 2012). This final step occurs through neurotrophin support deficiency from post-synaptic neurons, which secondarily induces neuronal autophagic death (McKnight et al., 2012). Similar but exaggerated mechanisms occur in brain pathologies including epilepsies and neurodegenerative disorders (Alzheimer's and Parkinson's diseases, neurometabolic disorders) which may exhibit aberrant axonal growth followed by neuronal autophagy, behavioral consequences, cognitive decline and seizures (Yan et al., 2012a, 2012b; Ebrahimi-Fakhari et al., 2014). Our partial GAMT-deficient cultures exhibited identical patterns with primary axonal hypersprouting paralleled by apoptosis decrease. Secondarily, while GAP43 was still overexpressed and apoptosis still diminished, non-apoptotic cell death was induced, probably through autophagy in neurons with GAA-induced superfluous axons and lacking post-synaptic neurotrophins.

Axonal hypersprouting may occur through GAA-induced slowing of Na^+/K^+ -ATPase (Zugno et al., 2004), leading to increased intracellular Ca^{++} triggering augmented expression (shown here)

and overactivation of Ca⁺⁺-dependent GAP43 (Dunican and Doherty, 2000), known to participate in axonal sprouting (Aungst et al., 2013).

GAMT RNAi led to expression alteration of genes of the GABA-ergic neurotransmission pathway. Cr and GAA are known to affect GABA-ergic neurotransmission as partial agonists or antagonists on post-synaptic GABA_AR (De Deyn et al., 1991; Neu et al., 2002; Cupello et al., 2008). We confirmed that GAA accumulation disturbs post-synaptic GABA_AR-expressing neurons, and demonstrate for the first time that their pre-synaptic GAD-expressing GABA-ergic partners appear affected. Thus, severe epilepsies in GAMT deficiency may not only be caused by direct GAA action on GABA_AR, but also by aberrant re-modeling of GABA-ergic circuitry through axonal hypersprouting, which was shown to play a role in epilepsy emergence and compensatory mechanisms balancing excitatory neurotransmission (Bausch, 2005; Buckmaster and Wen, 2011). GAA accumulation, by direct GABA_AR disturbances or by axonal hypersprouting followed by neuronal autophagy, may also affect the recently proposed role of Cr as neurotransmitter (Almeida et al., 2006; Peral et al., 2010; van de Kamp et al., 2013).

Diagnosis of GAMT deficiency and neonatal screening

GAMT deficiency is diagnosed in patients with intellectual disability/developmental delay or severe seizures once CNS Cr deficiency has been demonstrated by ¹H-MRS together with elevated GAA in blood or urine (Stöckler-Ipsiroglu et al., 2014). Every patient diagnosed so far showed negligible (0-4%) residual GAMT activity (Mercimek-Mahmutoglu et al., 2006, 2014). Our findings suggest that GAMT activity must be negligible to cause CNS Cr deficiency, as 15% residual expression did not generate Cr deficiency. However, GAMT residual expression was

insufficient to maintain normal GAA levels, and accumulated GAA without Cr deficiency was sufficient to produce irreversible effects on brain cells. Our results suggest that some patients with residual GAMT activity may be missed, escaping diagnosis due to lack of CNS Cr deficiency. Recent proposals for GAMT deficiency entry in neonatal screening programs by measure of GAA on dried blood spots (Mercimek-Mahmutoglu et al., 2012; El-Gharbawy et al., 2013; Pasquali et al., 2014) would therefore also help identify those patients with significant residual GAMT activity and allow their pre-symptomatic treatment (Schulze et al., 2006). This may also allow the detection of altered, toxic levels of GAA independently of GAMT deficiency, as recently observed for example in arginase deficiency (Amayreh et al., 2014).

Prevention of GAA toxicity by creatine supplementation

Our second striking result was the prevention of all observed GAA deleterious effects by Cr supplementation, despite GAMT deficiency. Cr supplementation, paralleled to scAAV2/GAMT-2 transduction, prevented axonal hypersprouting, natural apoptosis decrease, and secondary increase of non-apoptotic cell death. It also prevented GABA-ergic disturbances. While other neuroprotective mechanisms by Cr (Gualano et al., 2010) cannot be excluded, prevention of GAA effects probably occurred through negative feedback regulation of the first enzyme of Cr synthesis, AGAT, leading to GAA measures below control levels. AGAT feedback inhibition by Cr, though already known in kidney cells (Takeda et al., 1992), has never beforehand been demonstrated in AGAT-expressing brain cells (Braissant et al., 2008, 2010). The prevention of both GAA accumulation and its toxic effects by Cr supplementation despite GAMT deficiency, together with the prevention of the same toxic effects by Cr supplementation under direct

exposure to GAA, demonstrates the direct involvement of GAA in axonal hypersprouting and disturbed brain cell death in our model of partial GAMT deficiency by RNAi.

GAMT deficiency treatment requires life-long high Cr doses due to low BBB permeability for Cr (Braissant, 2012; Stöckler-Ipsiroglu et al., 2014). Associated GAA-lowering strategies (ornithine supplementation and arginine restriction; Schulze et al., 2001) strongly decrease plasma and cerebrospinal fluid GAA, but brain levels remain 10 times above normal values (Stöckler-Ipsiroglu et al., 2014). Our work suggests that finding new ways to increase Cr transport efficacy through BBB may correct GAA to control levels in GAMT-deficient CNS and significantly improve the disease outcome. One possibility would be the induction of the SLC6A8 transporter in the astrocytic feet surrounding BBB, which would greatly increase BBB permeability for Cr.

Conclusions

We have shown in 3D organotypic brain cell cultures that GAMT deficiency with significant residual enzymatic activity does not lead to Cr deficiency but generates sufficient GAA to irreversibly affect developing CNS. GAA primarily impacted neurons by axonal hypersprouting and apoptosis inhibition, followed by secondary non-apoptotic cell death induction. Future work will aim at better characterizing signaling pathways involved, disturbances in neurotransmission and cell death (apoptosis *versus* autophagy or necrosis). We could characterize some of the brain GAA-specific effects independently from Cr deficiency. Our results should stimulate the search for GAMT-deficient patients with significant residual GAMT activity, escaping Cr deficiency diagnosis but presenting symptoms of GAMT deficiency. These patients should be identified through newly proposed programs of neonatal screening by GAA measurement. Our work

finally suggests that facilitating Cr crossing through BBB may help normalizing brain GAA levels and further improve the outcome of GAMT deficiency.

Acknowledgments :

We thank Marc Loup, Alexandre Béguin and Catherine Pythoud for excellent technical work.

This work was supported by the Swiss National Science Foundation (grants n° 3100A0-116859 and 31003A-130278). The authors declare no competing financial interests.

References

- Almeida, L.S., G.S. Salomons, F. Hogenboom, C. Jakobs, and A.N. Schoffemeer. 2006. Exocytotic release of creatine in rat brain. *Synapse* 60:118-123.
- Almeida, L.S., N.M. Verhoeven, B. Roos, C. Valongo, M.L. Cardoso, L. Vilarinho, G.S. Salomons, and C. Kakobs. 2004. Creatine and guanidinoacetate: diagnostic markers for inborn errors in creatine biosynthesis and transport. *Mol. Genet. Metab.* 82:214-219.
- Amayreh, W., U. Meyer, and A.M. Das. 2014. Treatment of arginase deficiency revisited: guanidinoacetate as a therapeutic target and biomarker for therapeutic monitoring. *Dev. Med. Child Neurol.* 56:1021–1024.
- Aungst, S., P.M. England, and S.M. Thompson. 2013. Critical role of trkB receptors in reactive axonal sprouting and hyperexcitability after axonal injury. *J Neurophysiol* 109:813-824.
- Bausch, S.B. 2005. Axonal sprouting of GABAergic interneurons in temporal lobe epilepsy. *Epilepsy Behav.* 7:390-400.
- Béard, E., and O. Braissant. 2010. Synthesis and transport of creatine in the CNS: importance for cerebral functions. *J. Neurochem.* 115:297-313.
- Braissant, O. 2012. Creatine and guanidinoacetate transport at blood-brain and blood-cerebrospinal fluid barriers. *J. Inherit. Metab. Dis.* 35:655-664.
- Braissant, O. 2014. GAMT deficiency: 20 years of a treatable inborn error of metabolism. *Mol. Genet. Metab.* 111:1-3.

- Braissant, O., and H. Henry. 2008. AGAT, GAMT and SLC6A8 distribution in the central nervous system, in relation to creatine deficiency syndromes: a review. *J. Inherit. Metab. Dis.* 31:230-239.
- Braissant, O., E. Béard, C. Torrent, and H. Henry. 2010. Dissociation of AGAT, GAMT and SLC6A8 in CNS: relevance to creatine deficiency syndromes. *Neurobiol. Dis.* 37:423-433.
- Braissant, O., L. Cagnon, F. Monnet-Tschudi, O. Speer, T. Wallimann, P. Honegger, and H. Henry. 2008. Ammonium alters creatine transport and synthesis in a 3D-culture of developing brain cells, resulting in secondary cerebral creatine deficiency. *Eur. J. Neurosci.* 27:1673-1685.
- Braissant, O., H. Henry, M. Loup, B. Eilers, and C. Bachmann. 2001. Endogenous synthesis and transport of creatine in the rat brain: an in situ hybridization study. *Mol. Brain Res.* 86:193-201.
- Braissant, O., H. Henry, A.M. Villard, O. Speer, T. Wallimann, and C. Bachmann. 2005. Creatine synthesis and transport during rat embryogenesis: spatiotemporal expression of AGAT, GAMT and CT1. *BMC Dev. Biol.* 5:9.
- Braissant, O., H. Henry, A.M. Villard, M.G. Zurich, M. Loup, B. Eilers, G. Parlascino, E. Matter, O. Boulat, P. Honegger, et al. 2002. Ammonium-induced impairment of axonal growth is prevented through glial creatine. *J. Neurosci.* 22:9810-9820.
- Brosnan, J.T., and M.E. Brosnan. 2007. Creatine: endogenous metabolite, dietary, and therapeutic supplement. *Annu. Rev. Nutr.* 27:241-261.
- Buckmaster, P.S., and X. Wen X. 2011. Rapamycin suppresses axon sprouting by somatostatin interneurons in a mouse model of temporal lobe epilepsy. *Epilepsia* 52:2057-2064.

- Cagnon, L., and Braissant, O. 2008. Role of caspases, calpain and cdk5 in ammonia-induced cell death in developing brain cells. *Neurobiol. Dis.* 32:281-292.
- Cearley, C.N., L.H. Vandenberghe, M.K. Parente, E.R. Carnish, J.M. Wilson, J.H. Wolfe JH. 2008. Expanded repertoire of AAV vector serotypes mediate unique patterns of transduction in mouse brain. *Mol. Therapy* 16:1710-1718.
- Cupello, A., M. Balestrino, E. Gatta, F. Pellistri, S. Siano, M. Robello. 2008. Activation of cerebellar granule cells GABA(A) receptors by guanidinoacetate. *Neuroscience* 152:65-69.
- De Deyn, P.P., B. Marescau, and R.L. MacDonald. 1991. Guanidino compounds that are increased in hyperargininemia inhibit GABA and glycine responses on mouse neurons in cell culture. *Epilepsy Res.* 8:134-141.
- Diez, H., J.J. Garrido, and F. Wandosell. 2012. Specific roles of Akt iso forms in apoptosis and axon growth regulation in neurons. *PLoS One* 7:e32715.
- Duncan, D.J., and P. Doherty. 2000. The generation of localized calcium rises mediated by cell adhesion molecules and their role in neuronal growth cone motility. *Mol. Cell. Biol. Res. Com.* 3:255-263.
- Ebrahimi-Fakhari, D., L. Wahlster, G.F. Hoffmann, S. Kölker. 2014. Emerging role of autophagy in pediatric neurodegenerative and neurometabolic diseases. *Pediatr. Res.* 75:217-226.
- El-Gharbawy, A.H., J.L. Goldstein, D.S. Millington, A.E. Vaisnins, A. Schlune, B.A. Barshop, A. Schulze, D.D. Koeberl, and S.P. Young. 2013. Elevation of guanidinoacetate in newborn dried blood spots and impact of early treatment in GAMT deficiency. *Mol. Genet. Metab.* 109:215–217.

- Gualano, B., G.G. Artioli, J.R. Poortmans, and A.H. Lancha. 2010. Exploring the therapeutic role of creatine supplementation. *Amino Acids* 38:31-44.
- Honegger, P., and F. Monnet-Tschudi. 2001. Aggregating neural cell culture. In *Protocols for Neural Cell Culture*. S. Fedoroff, and A. Richardson, editors. Humana Press, Totowa. 199-218.
- Item, C.B., S. Stöckler-Ipsiroglu, C. Stromberger, A. Mühl, M.G. Alessandri, M.C. Bianchi, M. Tosetti, F. Fornai, and G. Cioni. 2001. Arginine:glycine amidinotransferase deficiency: the third inborn error of creatine metabolism in humans. *Am. J. Hum. Gen.* 69:1127-1133.
- Low, L.K., and Cheng H.J. 2006. Axon pruning: an essential step underlying the developmental plasticity of neuronal connections. *Phil. Trans. Royal Soc. London. B, Biol. Sci.* 361:1531-1544.
- Lowe, M., R.L. Faull, D. Christie, H. Waldvogel. 2014. The distribution of the creatine transporter throughout the human brain reveals a spectrum of creatine transporter immunoreactivity. *J. Comp. Neurol.* in press.
- McKnight, N.C., N. Mizushima, and Z. Yue. 2012. The cellular process of autophagy and control of autophagy in neurons. In *Autophagy of the Nervous System: Cellular Self-Digestion in Neurons and Neurological Diseases*. Z. Yue, and C.T. Chu, editors. World Scientific, Singapore. 3-35.
- Mercimek-Mahmutoglu, S., J. Ndika, W. Kanhai, T.B. de Villemeur, D. Cheillan, E. Christensen, N. Dorison, Hannig, Y. Hendriks, F.C. Hofstede, et al. 2014. Thirteen new patients with guanidinoacetate methyltransferase deficiency and functional characterization of nineteen novel missense variants in the GAMT gene. *Hum. Mut.* 35:462-469.

Mercimek-Mahmutoglu, S., Stoeckler-Ipsiroglu S., Adami A., Appleton R., Caldeira Araujo H., Duran M., Ensenauer R., Fernandez-Alvarez E., Garcia P., Grolik C., et al. 2006. GAMT deficiency: Features, treatment, and outcome in an inborn error of creatine synthesis. *Neurology* 67:480–484.

Mercimek-Mahmutoglu, S., G. Sinclair, S.J. van Dooren, W. Kanhai, P. Ashcraft, O.J. Michel, J. Nelson, O.T. Betsalel, L. Sweetman, C. Jakobs, et al. 2012. Guanidinoacetate methyltransferase deficiency: first steps to newborn screening for a treatable neurometabolic disease. *Mol. Genet. Metab.* 107:433-437.

Neu, A., H. Neuhoff, G. Trube, S. Fehr, K. Ullrich, J. Roeper, and D. Isbrandt D. 2002. Activation of GABA(A) receptors by guanidinoacetate: a novel pathophysiological mechanism. *Neurobiol. Dis.* 11:298-307.

Pasquali, M., E. Schwarz, M. Jensen, T. Yuzyuk, I. DeBiase, H. Randall, and N. Longo. 2014. Feasibility of newborn screening for guanidinoacetate methyltransferase (GAMT) deficiency. *J. Inherit. Metab. Dis.* 37:231-236.

Peral M.J., M.D. Vazquez-Carretero, and A.A. Ilundain. 2010. Na⁽⁺⁾/Cl⁽⁻⁾/creatine transporter activity and expression in rat brain synaptosomes. *Neuroscience* 165:53-60.

Renema, W.K., A. Schmidt, J.J. van Asten, F. Oerlemans, K. Ullrich, B. Wieringa, D. Isbrandt, and A. Heerschap. 2003. MR spectroscopy of muscle and brain in guanidinoacetate methyltransferase (GAMT)-deficient mice: validation of an animal model to study creatine deficiency. *Magn. Reson. Med.* 50:936-943.

- Salomons, G.S., S.J. van Dooren, N.M. Verhoeven, K.M. Cecil, W.S. Ball, T.J. DeGrauw, and C. Jakobs. 2001. X-linked creatine-transporter gene (SLC6A8) defect: a new creatine-deficiency syndrome. *Am. J. Hum. Gen.* 68:1497-1500.
- Schmidt, A., B. Marescau, E.A. Boehm, W.K. Renema, R. Peco, A. Das, R. Steinfeld, S. Chan, J. Wallis, M. Davidoff, et al. 2004. Severely altered guanidino compound levels, disturbed body weight homeostasis and impaired fertility in a mouse model of guanidinoacetate N-methyltransferase (GAMT) deficiency. *Hum. Mol. Genet.* 13:905-921.
- Schulze, A. 2003. Creatine deficiency syndromes. *Mol. Cell. Biochem.* 244:143-150.
- Schulze, A., and R. Battini. 2007. Pre-symptomatic treatment of creatine biosynthesis defects. *Subcell. Biochem.* 46:167-181.
- Schulze, A., F. Ebinger, D. Rating, and E. Mayatepek. 2001. Improving treatment of guanidinoacetate methyltransferase deficiency: reduction of guanidinoacetic acid in body fluids by arginine restriction and ornithine supplementation. *Mol. Genet. Metab.* 74:413-419.
- Schulze, A., T. Hess, R. Wevers, E. Mayatepek, P. Bachert, B. Marescau, M.V. Knopp, P.P. De Deyn, H.J. Bremer, and D. Rating. 1997. Creatine deficiency syndrome caused by guanidinoacetate methyltransferase deficiency: diagnostic tools for a new inborn error of metabolism. *J. Pediatr.* 131:626-631.
- Schulze, A., G.F. Hoffmann, P. Bachert, S. Kirsch, G.S. Salomons, N.M. Verhoeven, and E. Mayatepek. 2006. Presymptomatic treatment of neonatal guanidinoacetate methyltransferase deficiency. *Neurology* 67:719-721.

- Stöckler, S., O. Braissant, and A. Schulze. 2014. Creatine disorders. In *Physician's Guide to the Diagnosis, Treatment, and Follow-Up of Inherited Metabolic Diseases*. N. Blau, M. Duran, K.M. Gibson, and C. Dionisi-Vici, editors. Springer-Verlag, Berlin. 529-540.
- Stöckler, S., U. Holzbach, F. Hanefeld, I. Marquardt, G. Helms, M. Requart, W. Hänicke, and J. Frahm. 1994. Creatine deficiency in the brain: a new, treatable inborn error of metabolism. *Pediatr. Res.* 36:409-413.
- Stöckler-Ipsiroglu, S., C. van Karnebeek, N. Longo, G.C. Korenke, S. Mercimek-Mahmutoglu, I. Marquart, B. Barshop, C. Grolik, A. Schlune, B. Angle, et al. 2014. Guanidinoacetate methyltransferase (GAMT) deficiency: outcomes in 48 individuals and recommendations
- Tachikawa, M., and K. Hosoya. 2011. Transport characteristics of guanidino compounds at the blood-brain barrier and blood-cerebrospinal fluid barrier: relevance to neural disorders. *Fluids Barriers CNS* 8:13.
- Tachikawa, M., M. Fukaya, T. Terasaki, S. Ohtsuki, and M. Watanabe. 2004. Distinct cellular expressions of creatine synthetic enzyme GAMT and creatine kinases uCK-Mi and CK-B suggest a novel neuron-glial relationship for brain energy homeostasis. *Eur. J. Neurosci.* 20:144-160.
- Takeda, M., I. Kiyatake, H. Koide, K.Y. Jung, and H. Endou. 1992. Biosynthesis of guanidinoacetic acid in isolated renal tubules. *Eur. J. Clin. Chem. Clin. Biochem.* 30:325-331.
- Tenenbaum, L., A. Chtarto, E. Lehtonen, T. Velu, J. Brotchi, and M. Levivier. 2004. Recombinant AAV-mediated gene delivery to the central nervous system. *J. Gene Med.* 6Suppl1:S212-S222.

- Tran, C., M. Yazdanpanah, L. Kyriakopoulou, V. Levandovskiy, H. Zahid, A. Naufer, D. Isbrandt, and A. Schulze. 2014. Stable isotope dilution microquantification of creatine metabolites in plasma, whole blood and dried blood spots for pharmacological studies in mouse models of creatine deficiency. *Clin. Chim. Acta* 436C:160-168.
- van de Kamp, J.M., C. Jakobs, K.M. Gibson, and G.S. Salomons. 2013. New insights into creatine transporter deficiency: the importance of recycling creatine in the brain. *J. Inherit. Metab. Dis.* 36:155-156.
- Viau, K.S., S.L. Ernst, M. Pasquali, L.D. Botto, G. Hedlund, and N.Longo. 2013. Evidence-based treatment of guanidinoacetate methyltransferase (GAMT) deficiency. *Mol. Genet. Metab.* 110:255–262.
- Wallimann, T., M. Wyss, D. Brdiczka, K. Nicolay, and H.M. Eppenberger. 1992. Intracellular compartmentation, structure and function of creatine kinase isoenzymes in tissues with high and fluctuating energy demands: the 'phosphocreatine circuit' for cellular energy homeostasis. *Biochem. J.* 281:21-40.
- Wang, L., and F.Y. Mu. 2004. A Web-based design center for vector-based siRNA and siRNA cassette. *Bioinformatics* 20:1818-1820.
- Yan, X.X., Y. Cai, J. Shelton, S.H. Deng, X.G. Luo, S. Oddo, F.M. Laferla, H. Cai, G.M. Rose, and P.R. Patrylo. 2012a. Chronic temporal lobe epilepsy is associated with enhanced Alzheimer-like neuropathology in 3xTg-AD mice. *PLoS One* 7:e48782.
- Yan, X.X., Y. Cai, X.M. Zhang, X.G. Luo, H. Cai, G.M. Rose, and P.R. Patrylo. 2012b. BACE1 elevation is associated with aberrant limbic axonal sprouting in epileptic CD1 mice. *Exp. Neurol.* 235:228-237.

Zugno, A.I., R. Franzon, F. Chiarani, C.S. Bavaresco, C.M. Wannmacher, M. Wajner, and A.T.

Wyse. 2004. Evaluation of the mechanism underlying the inhibitory effect of guanidinoacetate on brain Na⁺, K⁺-ATPase activity. *Int. J. Dev. Neurosci.* 22:191-196.

Zugno, A.I., E.B. Scherer, P.F. Schuck, D.L. Oliveira, S. Wofchuk, C.M. Wannmacher, M.

Wajner, and A.T. Wyse. 2006. Intrastratial administration of guanidinoacetate inhibits Na⁺, K⁺-ATPase and creatine kinase activities in rat striatum. *Metab. Brain Dis.* 21:41-50.

Figure legends

Figure 1: AAV2-transduced GAMT deficiency in 3D organotypic developing brain cell cultures. (A) The three sequences selected for GAMT RNAi, with their respective location on the rat *Gamt* gene ORF. Ctrl-2 mismatched and scrambled are the GAMT-2 siRNA-derived negative controls. (B) Dual luciferase assay for selection of the best GAMT shRNA. Co-transfection of ROC cells with pRNAT-CMV3.2/Neo/GAMT-1/2/3/empty and psiCHECK-GAMT. GAMT-2 shRNA led to the best knockdown. (C) GAMT protein expression in ROC cell monolayer after pRNAT-CMV3.2/Neo/GAMT-2 transfection or AAV2/GAMT-2 transduction (MOI 300). GAMT knockdown specificity was tested by transfection with empty vector or the negative controls pRNAT-CMV3.2/Neo/mismatched/scrambled. GAMT-2 shRNA drove a specific GAMT protein knockdown, and AAV2 viruses efficiently transduced the RNAi effect. Western blotting experiment normalized with β -tubulin. (D) GAMT protein expression in 3D organotypic brain cell cultures at DIV8 (top), DIV18 (middle) and DIV28 (bottom) after scAAV2/GAMT-2 transduction (MOIs 100/300/1000). Mismatched and scrambled negative controls were used to evaluate RNAi specificity (MOI 1000). Western blotting experiments normalized with actin. (E) Single point comparative expression of GAMT protein at DIV8, 18 and 28 in a representative culture transduced by scAAV2/GAMT-2 (MOI 1000). The highest GAMT expression and the strongest GAMT knockdown were observed at DIV18 (MOI 1000, n=1). Western blotting experiment normalized with actin. Western blotting data presented in **B,C,D**: mean \pm s.e.m (n=6 in 1 out of 5 representative experiments). * P <0.05, ** P <0.01, *** P <0.001.

Figure 2: 3D organotypic brain cell cultures transduced by EGFP-expressing scAAV2. (A)

Normal development schemes of 3D organotypic brain cell cultures. Aggregates at DIV8, 18 and 28 are described, at low and high magnification. Cultures develop with neurons, astrocytes and oligodendrocytes in a stereotyped manner. Neuronal soma are located in aggregate centers, and mixed with numerous astrocytes and rare oligodendrocytes. Neurons differentiate by sending processes and particularly axons (red lines, including growth cone triangles) at the periphery where privileged synapses are established (aggregate periphery delimited in enlarged boxes by the external continuous and the dotted black lines). The external cell layer of aggregates is essentially composed of astrocytes and few oligodendrocytes. The detailed description of this culture system has been extensively explained (Honegger and Monnet-Tschudi, 2001; Braissant et al., 2002; Cagnon and Braissant, 2008). **(B)** EGFP native fluorescence in scAAV2-transduced brain cells in whole aggregates (line 1) or aggregate cryosections (lines 2-5) at DIV8 (column 1), 18 (column 2) and 28 (column 3), showing the increase of EGFP in both level of expression and number of positive cells. scAAV2 targeted neurons (line 3; co-labeling with NeuN), astrocytes (line 4; co-labeling with GFAP) and oligodendrocytes (line 5; co-labeling with GalC). Column 4: higher magnifications of the boxed regions in their respective lines. Scale bars: 100 μm (columns 1-3) and 20 μm (column 4). MOI: 1000 for every infected culture.

Figure 3: GAA accumulation but no Cr deficiency under partial GAMT deficiency.

Intracellular (black) and extracellular (grey) levels of Cr **(A)** and GAA **(B)** in control or scAAV2/GAMT-2-transduced cultures, with or without Cr supplementation (1 mM). While the awaited accumulation of GAA was observed in scAAV2/GAMT-2-transduced aggregates, no Cr deficiency could be observed under partial GAMT deficiency. Interestingly, GAA accumulation

was completely prevented by Cr supplementation in scAAV2/GAMT-2-transduced cultures. Mean \pm s.e.m (n=6 in 1 out of 3 representative experiments); intracellular: * P <0.05, ** P <0.01, *** P <0.001; extracellular: ^+P <0.05, ^{++}P <0.01, ^{+++}P <0.001.

Figure 4: Partial GAMT deficiency leads to axonal hypersprouting. (A) Immunofluorescence for p-NFM in axons of control or scAAV2/GAMT-2/mismatched/scrambled-transduced cultures, with or without Cr supplementation (1 mM). Panels on the right: higher magnifications of boxed regions highlighted in the DIV18 column; aggregate periphery delimited by the external continuous and the dotted lines. GAMT RNAi induced axonal hypersprouting which occurred peripherally and in aggregate centers (DIV8,18,28). Axonal hypersprouting was prevented by Cr co-treatment (1 mM). scAAV2/GAMT-2-transduction caused tissue loss at DIV28, observable as holes (asterisks). At DIV28, except for the specific axonal hypersprouting still observable in GAMT RNAi aggregates, a non-specific viral effect was seen in every other scAAV2-transduced conditions (GAMT RNAi + Cr, mismatched, scrambled) which led to p-NFM decrease as compared to controls. (B) Expression of total NFM (grey), p-NFM (black) and GAP43 in DIV18 and 28 cultures. NFM and GAP43 increase was specific at DIV18, and prevented by Cr co-treatment. The effect was still observable for GAP43 at DIV28, while scAAV2/GAMT-2-transduction with and without Cr co-treatment showed NFM and p-NFM decrease. Western blotting experiments normalized with actin. (C) Immunofluorescence for MAP2 in DIV18 cultures. No change in MAP-2 expression was observed. MOI: 1000 for every infected culture. Scale bars: 100 μ m (except enlarged boxes in **a**: 10 μ m). Histological data in **A,C**: evaluation of n=3 in 1 out of 4 representative experiments; western blotting data in **B**: mean \pm s.e.m (n=3 in 1 out of 4

representative experiments); total NFM: * $P < 0.05$, ** $P < 0.01$, *** $P < 0.001$; p-NFM: ⁺ $P < 0.05$, ⁺⁺ $P < 0.01$, ⁺⁺⁺ $P < 0.001$.

Figure 5: Partial GAMT deficiency does not affect glial cells. (A) Immunofluorescence for GFAP in astrocytes of control or scAAV2/GAMT-2/mismatched/scrambled-transduced cultures, with or without Cr supplementation (1 mM). GAA accumulation did not affect GFAP expression (DIV8,18). GAMT RNAi-specific tissue loss was observable as holes (DIV28; asterisks). A non-specific viral effect was seen at DIV28 only, leading to GFAP increase. (B) Western blotting analysis of GFAP in control or scAAV2/GAMT-2-transduced cultures, with or without Cr supplementation. As in A, no change in GFAP expression could be observed at DIV18, while at DIV28, all scAAV2/GAMT-2-transduced aggregates showed GFAP increased expression. (C) Immunofluorescence for GalC in oligodendrocytes of control or scAAV2/GAMT-2-transduced cultures, with or without Cr supplementation. GAMT RNAi did not affect GalC or the number of oligodendrocytes at either stage. (D) Immunofluorescence for MBP in control or scAAV2/GAMT-2/mismatched/scrambled-transduced cultures, with or without Cr supplementation (DIV28). Aggregate periphery delimited by the external continuous and the dotted lines. As in A, a non-specific viral effect was observed, showed by MBP decrease. (E) Western blotting analysis of MBP in control or scAAV2/GAMT-2-transduced cultures, with or without Cr supplementation (DIV18,28). No change in MBP expression could be observed at DIV18, while at DIV28 all scAAV2/GAMT-2-transduced aggregates showed MBP decrease. Western blotting experiments normalized with actin. MOI: 1000 for every infected culture. Scale bar: 100 μm . Histological data in A,C,D: evaluation of $n=3$ in 1 out of 4 representative

experiments; western blotting data in **B,E**: mean \pm s.e.m (n=3 in 1 out of 4 representative experiments); * P <0.05, ** P <0.01.

Figure 6: Partial GAMT deficiency primarily decreases normal developmental apoptosis, and secondarily induces non-apoptotic death of brain cells. (A) Fluorescent co-labeling of cell nuclei (DAPI; blue), whole dying (TUNEL; green) and apoptotic (cleaved caspase-3; red) cells in control or scAAV2/GAMT-2/mismatched/scrambled-transduced cultures, with or without Cr supplementation (1 mM). Aggregate periphery delimited by the external continuous and the dotted lines. At every stage, GAMT RNAi induced a decrease of naturally-occurring apoptosis (red), especially in aggregate centers (right of the dotted line). As expected, the number of naturally occurring apoptotic cells in control aggregates was lower in the more mature DIV28 stage than at DIV8 or 18. At DIV28, a specific GAMT RNAi-induced secondary increase in non-apoptotic dying cells was observed in aggregate centers (green-only TUNEL, without co-labeling by red activated caspase-3). These TUNEL-labeled dying cells at DIV28 surrounded the same tissue alterations illustrative of massive cell death as shown in **Figures 3A** and **4A**, and observable as holes (asterisks). These specific GAMT RNAi effects on cell death (both apoptotic and non-apoptotic) were prevented by Cr co-treatment. (B) Western blotting analysis of cleaved caspase-3 in control or scAAV2/GAMT-2-transduced cultures, with or without Cr supplementation. At every stage, cleaved caspase-3 was significantly decreased in scAAV2/GAMT-2-transduced cultures and Cr co-treatment prevented this effect. Western blotting experiments normalized with actin. MOI: 1000 for every infected culture. Scale bar: 100 μ m. Histological data in **A**: evaluation of n=3 in 1 out of 4 representative experiments; western blotting data in **B**: mean \pm s.e.m (n=3 in 1 out of 4 representative experiments); ** P <0.01.

Figure 7: Direct exposure to GAA resumes the effect of scAAV2-transduced partial GAMT deficiency, generating axonal hypersprouting and inhibiting apoptosis. Immunofluorescence analysis of p-NFM (**A**) and cleaved caspase 3 (**B**), as well as TUNEL labeling (**B**), in DIV18 controls and cultures exposed to 10 or 30 μ M GAA, with or without Cr supplementation (1 mM). At DIV18, direct GAA exposure generated a dose-dependent axonal hypersprouting, as well as inhibition of apoptosis. Both GAA-induced effects were prevented by Cr co-treatment. Intra- and extracellular measure of GAA (**C**) in DIV8 and DIV18 controls and cultures exposed to 10 or 30 μ M GAA. GAA-exposed cultures were able to take up GAA. Scale bar: 100 μ m (except enlarged boxes in **A**: 10 μ m). Histological data in **A,B**: evaluation of n=3 in 1 out of 4 representative experiments. Data in **C**: mean \pm s.e.m (n=3 in 1 out of 3 representative experiments); intracellular: ** P <0.01, *** P <0.001.

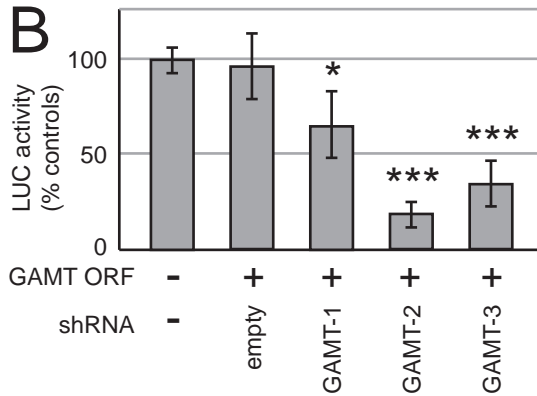
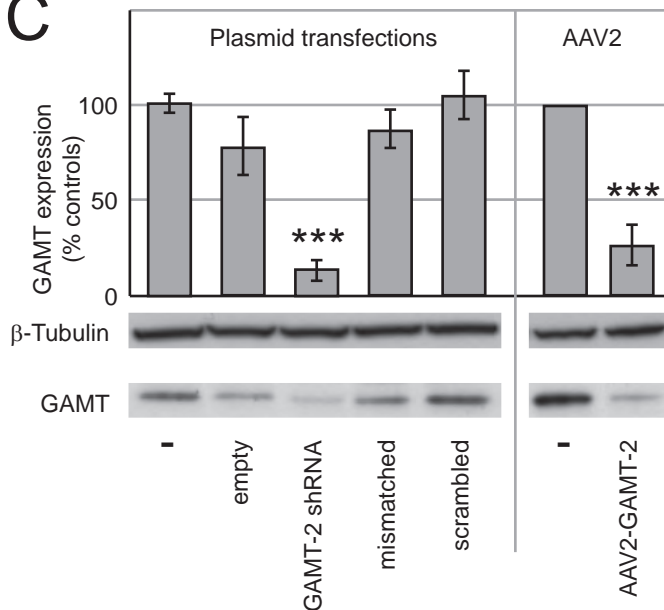
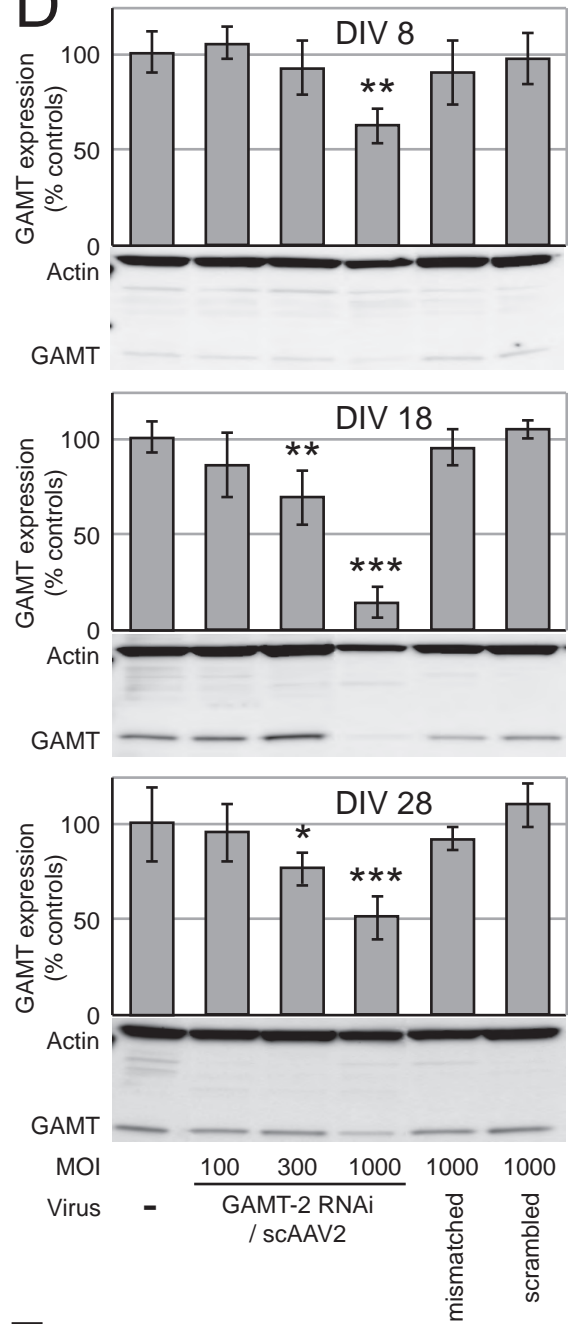
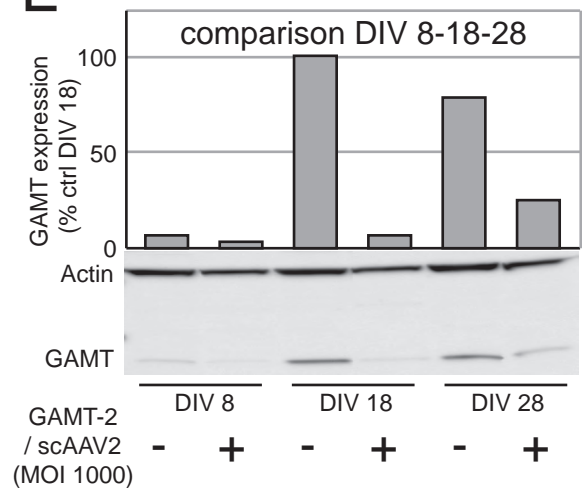
Figure 8: GAA accumulation under partial GAMT deficiency alters gene expression in GABA-ergic neurotransmission pathways. Immunofluorescence and western blotting analysis of GAD (**A**) and GABA_AR (**B**) in control and scAAV2/GAMT-2-transduced cultures, with or without Cr supplementation (1 mM). Increased GAD and GABA_AR expression was observed in the peripheral zone of scAAV2-GAMT-2-transduced and GAA-exposed aggregates at DIV18 and 28. This effect was prevented by Cr co-treatment. Aggregate periphery delimited by the external continuous and the dotted lines; positive neuronal cell bodies indicated by arrows. MOI: 1000 for every infected culture. Scale bar: 100 μ m. Western blotting experiments normalized with actin. Histological data in **A,B**: evaluation of n=3 in 1 out of 4 representative experiments; western blotting data in **A,B**: mean \pm s.e.m (n=3 in 1 out of 4 representative experiments);

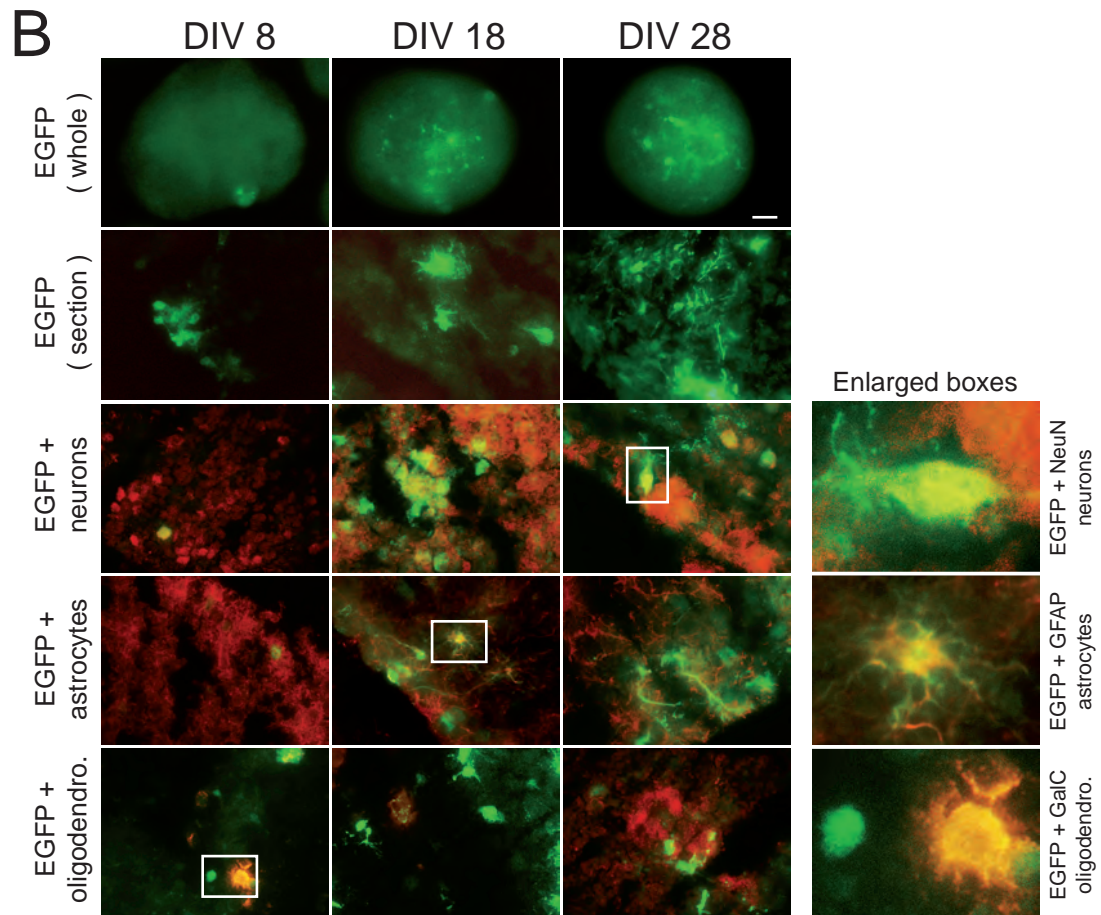
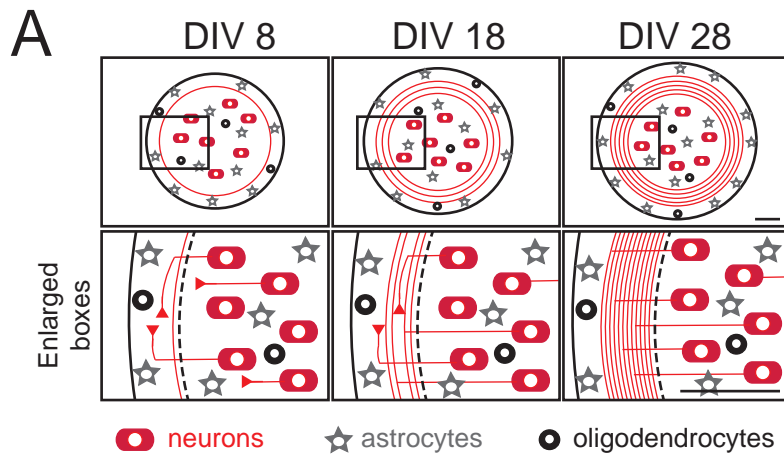
comparison to control: * $P < 0.05$, ** $P < 0.01$; comparison to GAMT RNAi or GAA exposure:
+ $P < 0.05$.

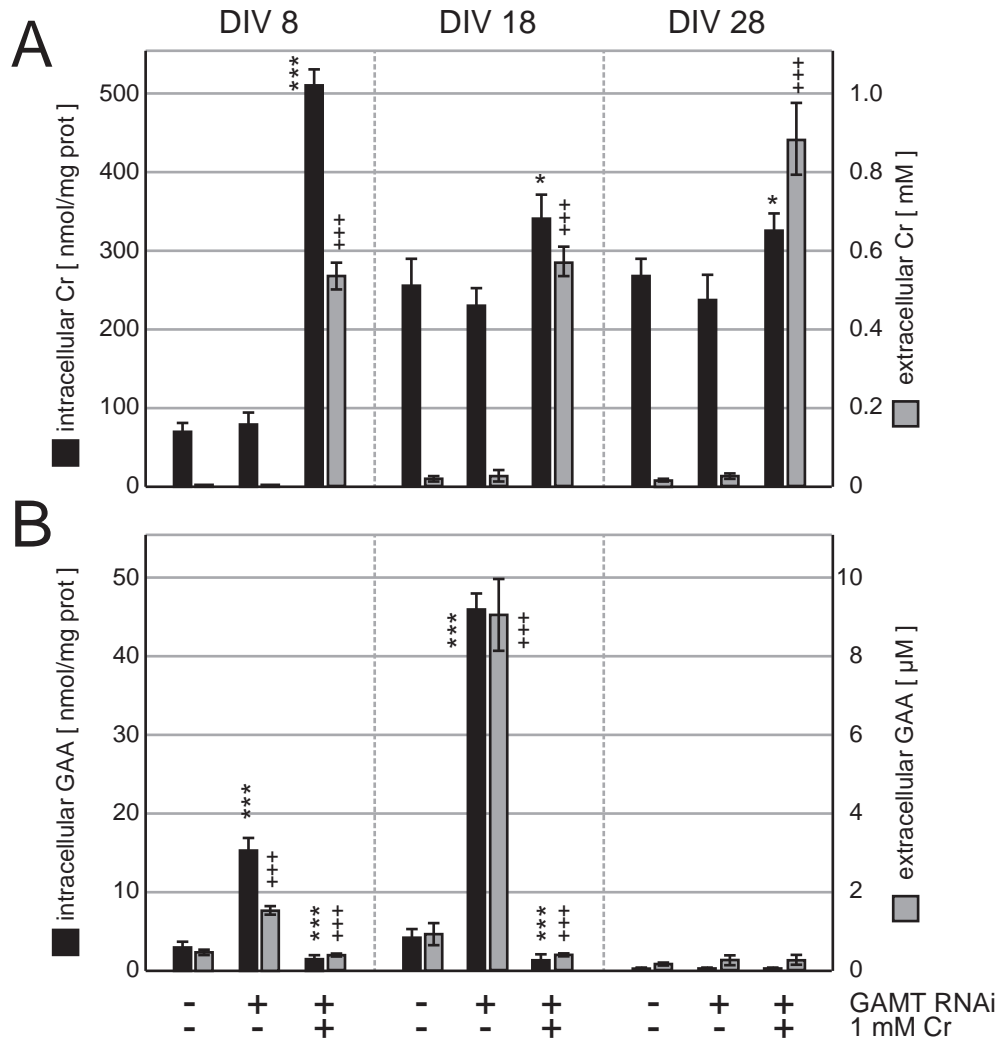
AsiRNAs **GAMT** (sense, 21 nt): ORF (nt)**GAMT-1** CTGGATTATTGAATGCAACGA 309-329**GAMT-2** GGAACTCATGAAGTCCAAGTA 576-596**GAMT-3** TGTCTGAAGAGACCTGGCACA 467-487

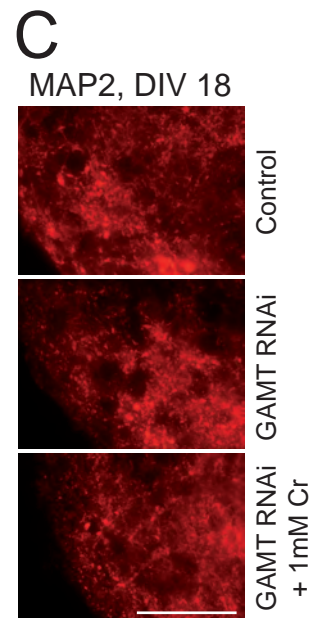
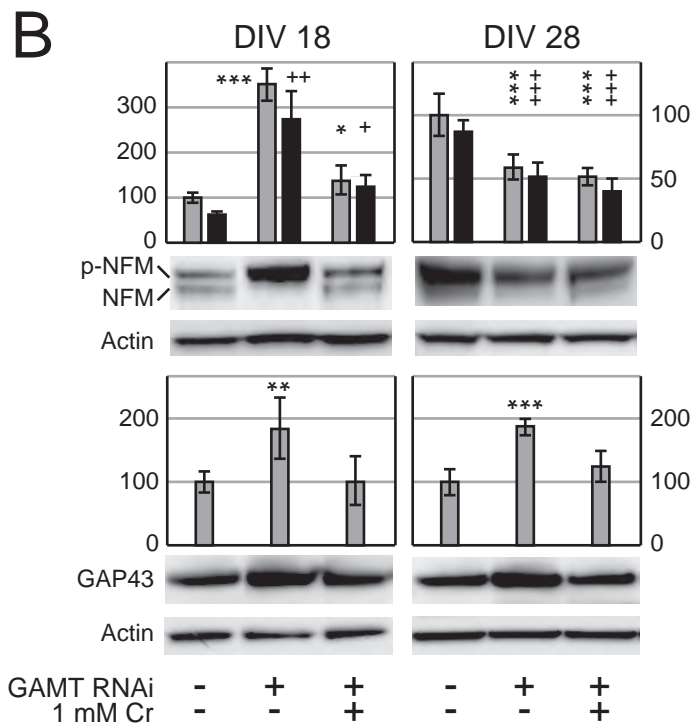
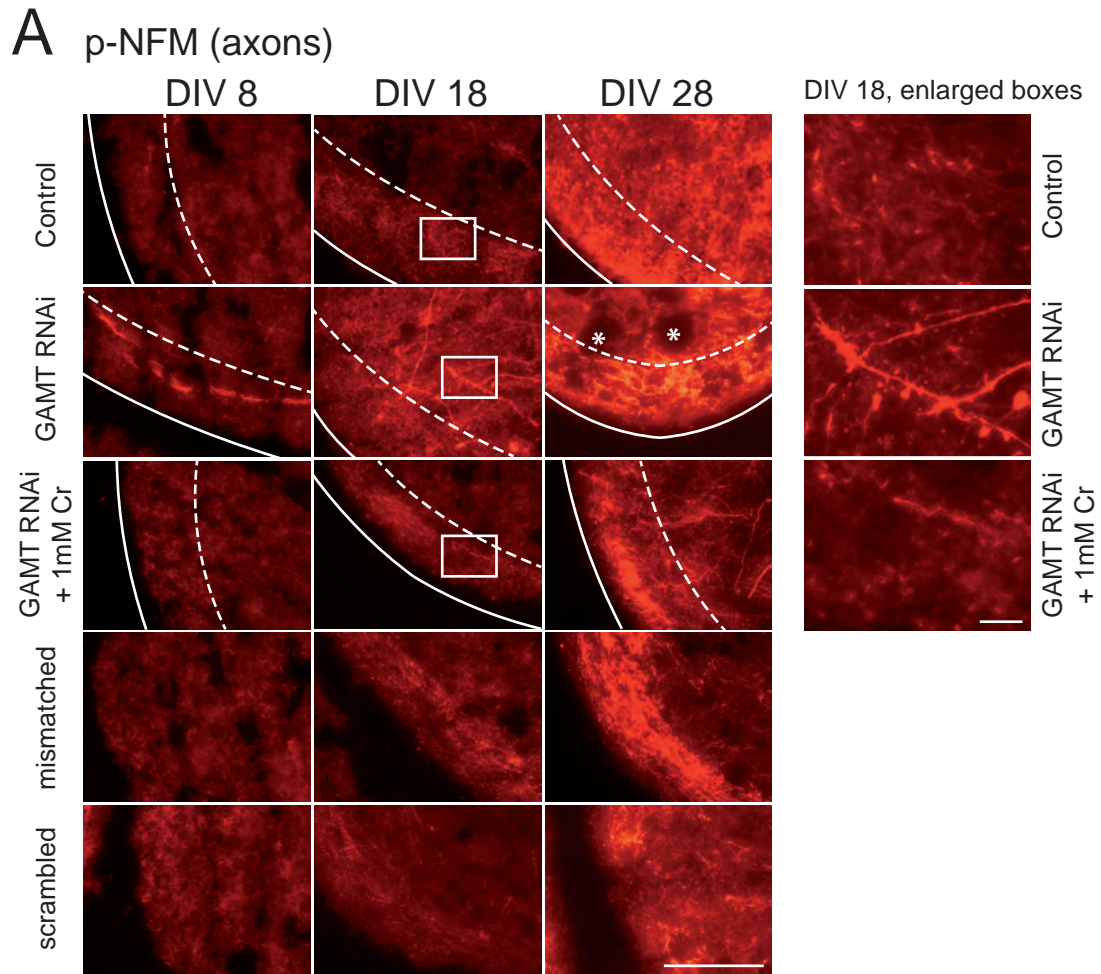
Ctrl-2 mismatched GGAACTCATCCAGTCCAAGTA

Ctrl-2 scrambled GTTCTCCTTACGCAATTAGGT

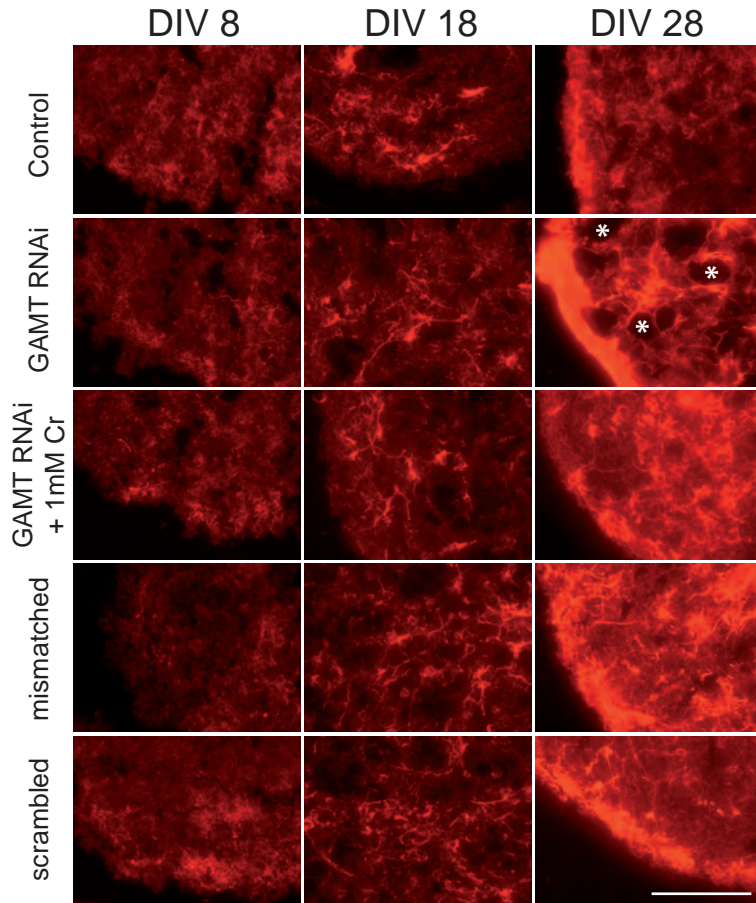
B**C****D****E**



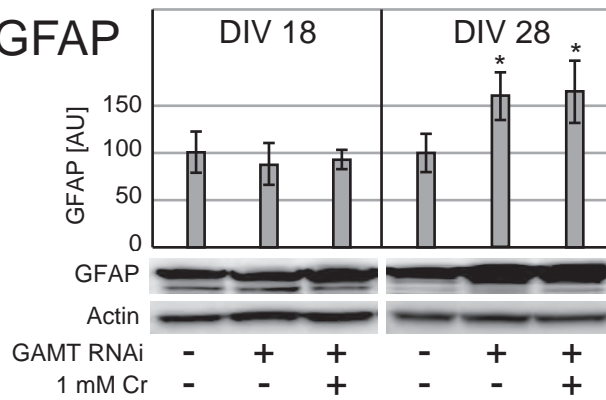




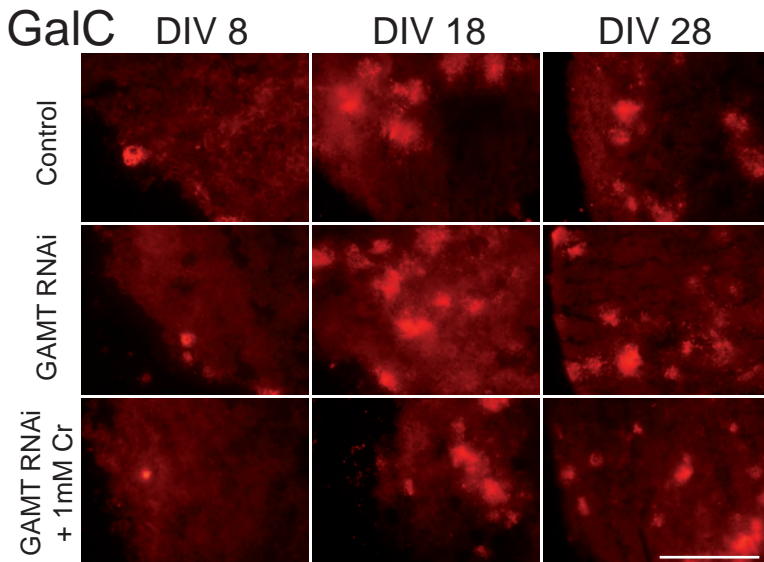
A GFAP



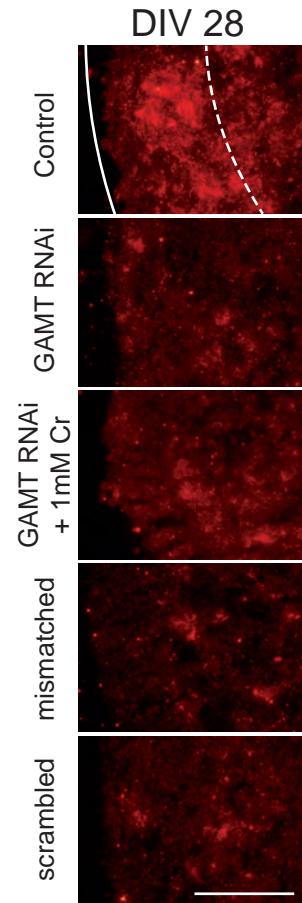
B GFAP



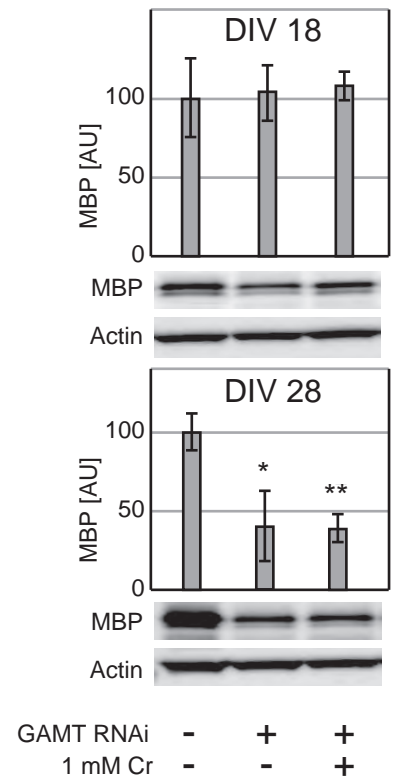
C GalC

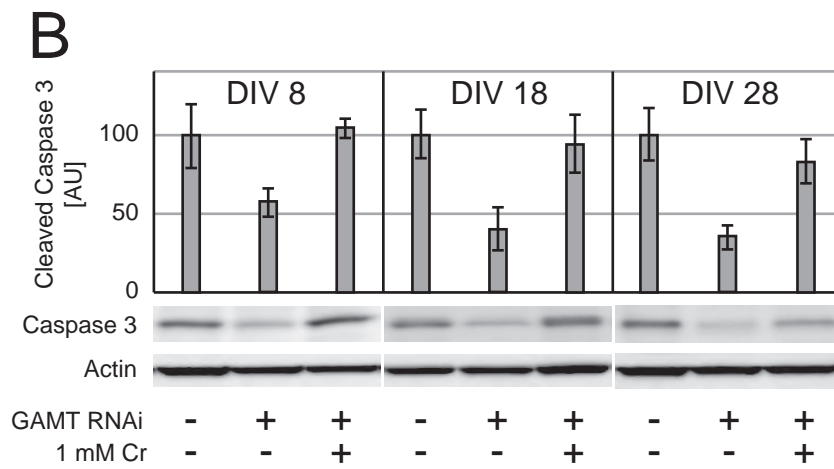
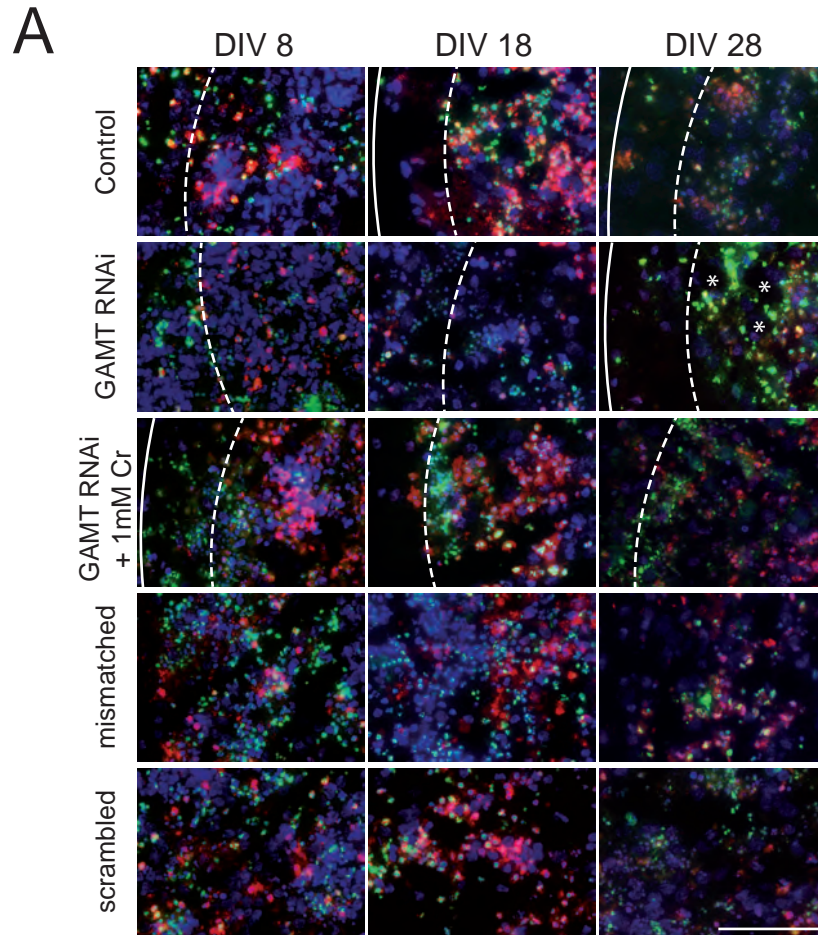


D MBP

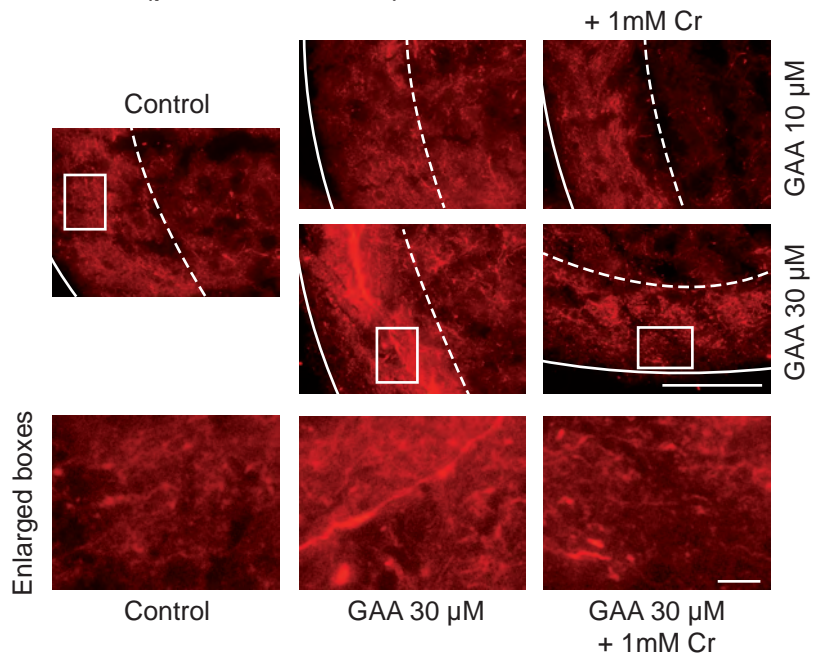


E MBP





A : axons (p-NFM; DIV18)



B : cell death (cleaved caspase 3 + TUNEL; DIV18)

